UNIVERSITY OF CALIFORNIA,
IRVINE

Sensing as it relates to behavior in fishes

DISSERTATION

submitted in partial satisfaction of the requirements
for the degree of

DOCTOR OF PHILOSOPHY

in Biological Sciences

by

Amberle McKee

Dissertation Committee:
Associate Professor Matthew J. McHenry, Chair
Associate Professor Donovan German
Professor Emeritus Timothey J. Bradley

2020

DEDICATION

To my loving husband, your love and support have been invaluable to me.
You are my biggest advocate and I am so excited to share this next adventure with you.

To my dear son, your presence in my life motivates me to do more than I could imagine.
I hope I can be a role model for you.

To my closest friends, you keep me sane and grounded.

To my family, you have encouraged me through it all.

TABLE OF CONTENTS

LIST OF FIGURES

ACKNOWLEDGMENTS

I would like to thank Dr. Matthew McHenry for his insights, support, and guidance during my dissertation. I came into your lab knowing little to nothing of engineering or programming, and leave with the knowledge and skillset to create complex physical experimental setups and to code anything my mind can imagine. Your guidance and encouragement helped me to grow as a scientist and as a person. I am extremely grateful to have you as an adviser.

I would like to thank my dissertation committee members, Dr. Timothy Bradley and Dr. Donovan German, and my advancement committee members, Dr. Catherine Loudan and Dr. Haithem E. Taha. I have valued the insights you bring, your extensive knowledge base and the difficult questions you pose. You pushed me to put my best foot forward. You were always there when I had a question and helped to connect me with resources. Thank you so much.

I would like to thank my undergrad mentees Naomi Carrillo and Phoebe Chen for their help with running experiments, providing animal care, and with data management.

I would also like to thank the faculty and graduate students in the physiology group of the Ecology and Evolutionary Biology Department for their support, constructive critiques, and collaborative advice.

This work was supported by grants from the National Science Foundation (IOS-1354842) and the Office of Naval Research (N00014-19-1-2035).

VITA

Amberle McKee

EDUCATION

Doctor of Philosophy in Biological Sciences — **2020**
University of California, Irvine — *Irvine, CA*

Bachelor of Science in Biological Sciences — **2014**
California State University, Long Beach — *Long Beach, CA*

RESEARCH EXPERIENCE

Graduate Research Assistant — **2014–2020**
University of California, Irvine — *Irvine, CA*

Postbaccalaureate Researcher — **Summber 2014**
Friday Harbor Laboratories, University of Washington — *Friday Harbor, WA*

Undergraduate Research Assistant — **2010–2014**
California State University, Long Beach — *Long Beach, CA*

TEACHING EXPERIENCE

Teaching Assistant — **2014–2020**
University of California, Irvine — *Irvine, CA*

GUEST LECTURES

Life in Microgravity — **Winter 2017**
University of California, Irvine — *Irvine, CA*

A Pattern of Good Behavior (Research) — **Fall 2015**
California State University, Long Beach — *Long Beach, CA*

JOURNAL PUBLICATIONS

3. McKee, A., MacDonald, I. Farina, S., and Summers, A. 2015. Undulation frequency affects burial performance in living and model flatfishes. Zoology. 119(2):75-80

2. McKee, A. A., Newton, S. M., Carter, A. J. R. 2014. Influence of inbreeding on female mate choice in two species of Drosophila. Journal of Insect Behavior. 27:613-625

1. McKee, A., Voltzow, J., and Pernet, B. 2013. Substrate attributes determine gait in a terrestrial gastropod. Biological Bulletin. 224:53-61

CONFERENCE PRESENTATIONS

10. McKee, A., Soto, A.P., Chen, P., and McHenry, M. J. 2020. The role of vision and flow sensing in schooling behavior. 15-minute oral presentation. Conference for the Society for Integrative and Comparative Biology, Austin, TX.

9. McKee, A., McHenry, M. J. 2019. How zebrafish use visual cues to evade predation. 15-minute oral presentation. Conference for the Society for Integrative and Comparative Biology, Tampa, FL.

8. McKee, A., McHenry, M. J. 2017. Growth changes the escape response to visual looming stimuli in zebrafish. 15-minute oral presentation. Conference for the Society for Integrative and Comparative Biology, New Orleans, LA.

7. McKee, A., McHenry, M. J. 2016. Growth changes the escape response to visual looming stimuli in zebrafish. 5-minute oral presentation. Southwestern Organismal Biology SICB Southwest Regional Meeting, Fullerton, CA.

6. McKee, A., McHenry, M. J. 2016. A high-throughput method for identifying responses to visual stimuli. Poster. Conference for the Society for Integrative and Comparative Biology, Portland, OR.

5. McKee, A., MacDonald, I. Farina, S., and Summers, A. 2015. Body undulation frequency affects burial performance in living and model flatfishes. 15-minute oral presentation. Conference for the Society for Integrative and Comparative Biology, West Palm Beach, FL.

4. McKee, A. A., Newton, S. M., Carter, A. J. R. 2014. Influence of inbreeding on female mate choice in two species of Drosophila. Poster. Conference for the Society for Integrative and Comparative Biology, Austin, TX.

3. McKee, A., Voltzow, J., and Pernet, B. 2013. Substrate attributes determine gait in a terrestrial gastropod. 5-minute oral presentation. Southwest regional conference for the Society for Integrative and Comparative Biology. UC Riverside.

2. McKee, A., Voltzow, J., and Pernet, B. 2013. Substrate attributes determine gait in a terrestrial gastropod. 10-minute oral presentation. Statewide Student Research Competition. CSU Long Beach and CSU Pomona.

1. McKee, A., Voltzow, J., and Pernet, B. 2013. Substrate attributes determine gait in a terrestrial gastropod. Poster. Conference for the Society for Integrative and Comparative Biology, San Francisco, CA.

OUTREACH

Lab Tour Guide **Spring 2017 and 2019**
University of California, Irvine *Irvine, CA*

Online Tutorials Creation **2015-2020**
University of California, Irvine *Irvine, CA*

Marine Lab Volunteer Caretaker **2009-2014**
California State University, Long Beach *Long Beach, CA*

Deckhand and Educator **2011-2012**
Children's Maritime Foundation *Long Beach, CA*

ABSTRACT OF THE DISSERTATION

Sensing as it relates to behavior in fishes

By

Amberle McKee

Doctor of Philosophy in Biological Sciences

University of California, Irvine, 2020

Associate Professor Matthew J. McHenry, Chair

Fish use their sensory systems to detect and engage with the world around them. Fish use different sensory cues from their environment to direct their own behaviors. Understanding how these cues affect the behavior of fish guides our thinking about fish behaviors. I studied three sensory systems in fish (vision, the lateral line, and the vestibular system) in the context of two behaviors important to fish (predator evasion and schooling).

My first dissertation chapter explored the use of vision in predator evasion. I created an automated experimental setup that projected looming visual stimuli of different approach velocities on the wall of a tank that contained an experimental fish. By analyzing the escape response of the fish in reaction to these stimuli, I was able to discern the threshold-visual angle (and rate of change of this angle) to which the fish were likely responding. I then ran experiments with live predators and found strong evidence that these threshold stimuli were accurate. Lastly, I used a mathematical model to explore the functional significance of these threshold stimuli. This model predicted that these threshold stimuli were most useful to the fish when the predator is slower than the prey. This work demonstrates how fish may use the threshold-visual angle (and angle rate) to evade predators.

My second dissertation chapter explored how fish use their lateral line and vestibular systems to detect flows which may indicate an approaching predator. The lateral line contains two

types of flow sensors: canal neuromasts (CNs), which detect pressure differences along the body that correlate with the acceleration of water flow, and superficial neuromasts (SNs), which detect the velocity of water flow with respect to the body. The vestibular system is a sensory system that detects the linear and rotational acceleration of the body. Using a neomycin sulfate bath, I was able to temporarily ablate the CNs and SNs on fish, leaving only the vestibular system functional. Using a more precise technique with neomycin sulfate, I was able to temporarily ablate the SNs, leaving the CNs largely intact. Thus, I created three groups of fish: those with their lateral lines intact (CNs+SNs), those with only their SNs ablated (CNs-only), and those with their lateral lines completely ablated (no-LL). I exposed each of these groups to a randomized set of flows and used the frequency of escape as a proxy for detection of the flow stimulus. I found that fish were able to escape from these flows with no lateral line, indicating the use of their vestibular system. Additionally, I found the CNs+SNs had an increased probability of detection over CNs-only and no-LL. This study demonstrates that fish are capable of using multiple sensory systems to detect flow stimuli.

My third chapter explored the use of the lateral line and vision in fish schooling behaviors. I recorded schools of five fish swimming after adjusting to different light levels. By measuring the distance between neighbors and the amount of polarization in the group, I was able to determine how well fish were able to school at each light level. I found that a minimum illuminance of >1.5 lux allowed fish to swim with sufficient polarization and distance between neighbors to be schooling. I then repeated the experiment with fish whose lateral line I had chemically ablated with neomycin sulfate. I found that these fish still schooled, but with a lower polarization and increased distance between neighbors. These results demonstrate that vision is required for schooling, and flow sensing modulates the quality of the schooling behavior.

Chapter 1

The strategy of predator evasion in response to a visual looming stimulus in zebrafish (*Danio rerio*).

1.1 Abstract

A diversity of animals survive encounters with predators by escaping from a looming visual stimulus. Despite the importance of this behavior, it is generally unclear how visual cues facilitate a prey's survival from predation. Therefore, the aim of the present study was to understand how the visual angle subtended on the eye of the prey by the predator affects the distance of adult zebrafish (*Danio rerio*) from predators. We performed experiments to measure the threshold visual angle and mathematically modeled the kinematics of predator and prey. We analyzed the responses to the artificial stimulus with a novel approach that calculated relationships between hypothetical values for a threshold-stimulus angle and the latency between stimulus and response. These relationships were verified against the

kinematic responses of zebrafish to a live fish predator (*Herichthys cyanoguttatus*). The predictions of our model suggest that the measured threshold visual angle facilitates escape when the predator's approach is slower than approximately twice the prey's escape speed. These results demonstrate the capacity and limits to how the visual angle provides a prey with the means to escape a predator.

1.2 Introduction

Evasive prey survive an encounter with a predator when they successfully execute an escape in response to a threatening sensory cue. Throughout this interaction, the distance between predator and prey affects both sensory information and the prey's prospects for survival [77, 16, 28, 66, 82, 87]. Fishes respond to a looming visual stimulus with a 'fast-start' escape response [69, 23, 27, 83] with a direction determined by the relative size and timing of muscle contractions on either side of the body [32]. It is unclear how visual cues facilitate this escape at sufficient proximity for prey survival. Therefore, the aim of the present study was to measure the visual cues that stimulate an escape response and to examine their effect on the distance from predators in zebrafish (*Danio rerio*, Hamilton, 1922).

The effects of a threatening visual stimulus can be studied under controlled experimental conditions. Looming may be simulated by projecting an expanding circle upon the wall, floor, or ceiling of a holding tank. In response, prey will generally initiate an escape if the circle's expanse is sufficiently rapid and large. A number of behavioral studies have considered the particular cue that triggers an escape by recording its timing relative to the projected stimulus in a diversity of animals that includes crabs [64], insects [2, 72], primates [73, 13], and birds [88]. Contemporary studies on fishes suggest that a threshold value of the visual angle offers the most robust predictor of an escape, within a range of approach velocities [83, 27, 69, 6]. The visual angle is the angle subtended on the eye by each of the

lateral margins of the looming stimulus (Fig. 1.1B). The fast-start is characterized by the body rapidly curling into a 'C' shape and then unfurling to accelerate [90]. In piscivorous interactions, this escape is commonly faster than the speed of the approaching predator, which often brake as they approach the prey, perhaps as a measure to coordinate a suction-feeding strike [40, 41, 77, 80]. As a consequence, the minimum distance between predator and prey is often achieved shortly after escape initiation. In this context, 'minimum distance' refers to smallest distance attained over time.

Resolving the threshold-stimulus angle poses a challenge for experimentalists because it is generally unknown how much time transpires between the threshold-stimulus and its response. This latency is due to the neurophysiological integration of the visual stimulus and the formulation of a motor response. In the absence of physiological measurements, this latency has been assumed by experimentalists to be either negligible or it has been approximated as a fixed parameter. Differences in this approximation have the potential to yield contrasting results for the threshold-stimulus angle. This is largely due to the visual angle increasing at a nonlinear rate when a predator approaches at a constant velocity. Because of this nonlinearity, small differences in the estimated latency can suggest very different values for the threshold. Indeed, the literature offers a variety of values of the threshold-simulus angle based on different latency values [24, 83, 27, 69].

The threshold-stimulus angle for an escape response has a direct influence on the evasive strategy of a prey fish. Evasion strategies are thought to be either unpredictable or optimized in some manner [15, 63, 25, 26, 47, 91]. The leading ideas for optimal evasion strategy are based on a differential game theory known as the homicidal chauffeur [47], which has been applied to fish predator-prey interactions [76, 91]. This theory includes calculations of the minimum distance (with respect to time) of a prey from a predator approaching from a fixed direction at a constant speed. Prey seek to keep this minimum distance as large as possible with an optimal strategy. The minimum distance depends principally on the relative speed

of the predator and prey and the distance between them at the start of the escape. This escape distance is dictated by the threshold-stimulus angle.

The present study measured the threshold-stimulus angle in zebrafish and considered its effect on the minimum distance. We hypothesized that zebrafish escape at a threshold that permits sufficient distance from a predator to evade capture. We developed an approach that is novel in a few respects to address some of the technical challenges for a study of this kind. We obtained a sufficient number of experiments without animal habituation with a computer-automated setup that altered its protocol according to the behavioral responses of the animal. The second challenge was to find values for both the threshold visual-stimulus angle and latency that are predictive of the behavior (also for the rate of change of the visual angle, see Supplemental Materials). We developed an analytical approach that uses the statistical power of all of our experiments to resolve a relationship between the threshold-stimulus angle and the latency. We additionally performed experiments on a fish predator, a red Texas cichlid (*Herichthys cyanoguttatus*), to validate the values for the threshold-stimulus angle . Finally, we applied a game-theoretical framework to consider the strategic implications of this threshold.

1.3 Methods

1.3.1 Animal husbandry

We raised wild-type (AB line) zebrafish (*Danio rerio*) according to standard procedures [92]. The fish were held in a flow-through tank system (Aquatic Habitats, Apopka, FL, USA) in 3 L containers at 27°C and fed daily with a 14:10 h light:dark cycle. The cichlid (*Herichthys cyanoguttatus*, 15 cm total length) that we used as a predator was obtained from a fish store and was held separately from the zebrafish at 25°C on the same light cycle

and fed daily. All rearing and experimental protocols were conducted with the approval of the Institutional Animal Care and Use Committee at the University of California, Irvine (Protocol #AUP-17-012).

1.3.2 Responses to a projected looming stimulus

We recorded the behavioral responses of 56 zebrafish exposed to a projected looming stimulus. Individual fish were placed in a rectangular clear acrylic tank (7.5 cm x 18.5 cm floor, water depth of 7 cm). The walls were angled outward by 4 deg to minimize their appearance when viewed from below. The tank was elevated above a mirror tilted at a 45 deg angle from the view of a high-speed camera (Photron FastCam SA2, San Diego, CA, USA set to 1000 fps at 1280 x 640 pixels) with a 55 mm macro lens (Nikon Corporation, Melville, NY, USA). The lens was positioned at a distance from the closest tank wall (54 cm) that allowed us to view the entire underside of the tank through the mirror. Three infrared lights (IR Illuminator CM-IR200, CMVision, Houston, Tx, USA; wavelength: 850 nm, illuminance: 10 lux) were placed above the tank and a plastic lid placed on the tank served as a light diffuser. Another diffuser was affixed to the wall of the tank facing the camera and a small projector (Brookstone 801143 Texas Instruments, Merrimack, NH, USA) was focused on this surface to present the looming stimulus (Fig. 1.1A).

The experiments were conducted with an automated system operated by two computers to allow for high-throughput experimentation. One computer was used to turn on the IR lights, initiate recording by the video camera, and to project the looming stimulus. These tasks were achieved with custom software scripted in MATLAB (version R21015a, Mathworks, Natick, MA, USA). The IR lights were controlled using an analog output channel from a data acquisition device (DAQ, National Instruments NI DAQ USB-6009, Austin, TX, USA) attached to a solenoid switch controlling the power to the lights. The DAQ also

triggered the camera, which was configured by the second computer running the camera software (Photron FASTCAM Viewer 3, San Diego, CA, USA). After an experiment, the second computer also ran custom MATLAB software to perform a kinematic analysis on the video recording to determine whether the fish responded to the stimulus. The two computers shared a network connection, which allowed the kinematic results of an experiment determined by one computer to be communicated to the other computer, which controlled the stimulus. This allowed the result of an experiment to affect the decision about the following experiment. This automated setup offered the additional benefit of eliminating the presence of an experimentalist that could influence the fish's behavior.

Our automated experiments followed a protocol that aimed to maximize the number of responses we recorded from an individual fish (Fig. 1.1C). The zebrafish was permitted to acclimate (2 hrs) prior to the first experiment and then experiments were performed once every hour, which pilot experiments demonstrated was a long-enough interval to prevent habituation [71]. Before each experiment, IR illumination was turned on 2 min prior to the presentation of a visual stimulus. The stimulus initially consisted of a small dark circle on a white field that was animated with lateral oscillations for 3 s to attract the attention of the fish. The circle then expanded in diameter until it reached its final size, which completely enveloped the screen. The camera was triggered to begin recording as the circle commenced expansion and to record for a duration of 3.99 s. Our analysis software automatically determined whether the fish responded by tracking the velocity of the center of the body. If the fish responded, a different stimulus was presented in the next experiment. Otherwise, fish were assumed not to have seen the stimulus and the same stimulus was repeated without the one hour delay to ensure the stimulus was visible to the fish during the recording. This process continued until the fish had been exposed to 8 unique stimuli and 2 controls (no stimulus shown) or until 24 hrs had transpired.

The rate of change of the diameter of the looming stimulus was varied to simulate a virtual predator approaching at a variety of fixed speeds. This virtual predator was assumed to have a circular appearance of fixed diameter ($S_{\text{vir}} = 30\,\text{cm}$) and to move toward the screen at a constant speed (u_{vir}). If one assumes that the observer maintains their distance from the wall ($d_{\text{wall}} = 2\,\text{cm}$) upon which the stimulus is projected, then the diameter of the projected circle (S_{wall}) may be calculated through an application of similar triangles:

$$\frac{S_{\text{vir}}}{d_{\text{vir}}} = \frac{S_{\text{wall}}}{d_{\text{wall}}}, \tag{1.1}$$

where d_{vir} is the distance between the prey and virtual predator, which may be calculated as $d_{\text{vir}} = d_{\text{vir},0} - u_{\text{vir}}t$. The initial distance of the virtual predator ($d_{\text{vir},0}$) was determined with Eqn. 1.1 using the value for the diameter of the attractive stimulus ($S_{\text{wall},0} = 5\,\text{mm}$). Our series of experiments projected stimuli intended to simulate virtual predators that approach at the following velocities: 19.35 cm s^{-1}, 25.8 cm s^{-1}, 32.25 cm s^{-1}, 38.7 cm s^{-1}, 45.15 cm s^{-1}, 51.6 cm s^{-1}, 58.05 cm s^{-1}, and 64.5 cm s^{-1}. Expressed by the ratio of the stimulus radius to its approach velocity [34], these stimuli ranged from 230 ms to 780 ms. However, the prey fish was free to move in these experiments which violates the assumptions of a fixed distance and position of the viewer. We therefore measured the realized visual angle to which the fish were exposed in each experiment, as detailed below.

1.3.3 Kinematic analysis

We measured the visual angle (θ) to which the fish were exposed prior to their escape response. This was found from measurements of the fish's position from our video recordings with a MATLAB program that first found the body of the fish as a dark area of pixels by thresholding each video frame. The fish was differentiated from pixels of similar intensity by its area and the midline of the body was found as a line of pixels furthest from the periphery

of the body using distance mapping (the 'bwdist' function in MATLAB). The greater width of the body at its anterior end differentiated it from the posterior end of the body. The position of the fish's eyes were identified by their consistent distance from the rostrum. We calculated the visual angle (θ) presented by the looming stimulus using the center of the eye and the width of the dark circle (Fig. 1.1B) for all frames in which the circle was within the eye's field of view [66]. Owing to the relatively modest overlap in the visual field of the two eyes, the stimulus rarely was presented within view of both eyes. In such instances, we considered only the visual angle of greater magnitude. We examined only those experiments that successfully elicited a fast start where the body of the fish curled into a 'C' shape prior to its acceleration and we pooled the measurements from all fish.

We used a novel analytical method to determine the relationship between the threshold-stimulus angle and latency that was most consistent with our experimental results. Each experiment provided measurements of the visual angle and the response time (t_{resp}), the moment when the escape response was initiated. From these measurements, we performed a series of calculations to determine the threshold time (t_{thresh}), the moment when the stimulus reached threshold, and the value of the threshold-stimulus angle (θ_{thresh}). We considered a range of hypothetical values for the threshold-stimulus angle and for each value, the threshold time was calculated as the moment at which the measurements of visual angle exceeded the threshold (Fig. 1.2A). Such calculations were performed to yield a relationship between the values of threshold time and response time for all experiments (Fig. 1.2B). If the latency between stimulus and response (t_{lat}) is consistent among experiments, then one should predict this relationship to be linear, with a slope of unity (i.e., $t_{\text{resp}} = t_{\text{thresh}} + t_{\text{lat}}$). For each hypothetical value of the threshold-stimulus angle , we calculated values for the threshold time among all experiments and performed a least-squares linear fit for the intercept for an assumed a slope of unity. We used the coefficient of determination (R^2) as a metric of the fit of this relationship to the data. This was achieved for 100 values at equal intervals for the visual angle ($0.5\,\text{deg} \leq \theta_{\text{thresh}} \leq 25.0\,\text{deg}$). The product of this process was a relationship

between the threshold-stimulus angle and latency that matched our experimental results and an indication of which threshold values offered the best fit to the data. This general approach may be applied to other sensory cues, such as the rate of change in the visual angle (see Supplemental Materials).

1.3.4 Responses to a live predator

We compared the responses to a projected stimulus to those elicited by a live cichlid predator (*Herichthys cyanoguttatus*). We positioned a high-speed video camera above a cylindrical tank ($\varnothing$ = 90 cm, 760 L, Fig. 1.1D), which was surrounded with a tarp to conceal the experimentalist. The cichlid was placed in the tank and allowed to acclimate for 2 hrs before we introduced a zebrafish to the tank. The camera recorded continuously on a loop until manually-triggered to save at the end of an escape response from the zebrafish. This escape generally occurred after several minutes of the zebrafish's introduction. Two escapes were recorded from each of 48 zebrafish and the cichlid never succeeded in capturing these prey.

The videos were manually digitized with ImageJ (version 1.52a, Wayne Rasband, National Institutes of Health, USA) to measure the coordinates of the rostrum and tail of both the cichlid predator and the zebrafish. From these coordinates, we calculated the visual angle between the anterior end of the zebrafish and the span of the cichlid's body (Fig. 1.1E). These coordinates were obtained for each frame from at least 150 ms prior to when the zebrafish initiated a C-start escape until the zebrafish either was coasting or swimming in its ultimate direction ($\sim$ 50 ms after the end of Stage 2).

We used the results of these experiments as an indication of how the responses to the projected stimulus applied to encounters with a live predator. For each experiment with the cichlid, we considered the values for the visual angle prior to an escape as the possible values that triggered the response. For each of these values, we calculated the time between

the time of the possible trigger and the escape time and used this as our proposed latency. This generated a range of hypothetical values for both the threshold and latency among all experiments. We compared these values against the latency and threshold values obtained in response to the projected stimulus. We considered overlapping values from the two types of experiments as indication of the responses that best apply to a live predator for zebrafish.

1.3.5 Mathematical modeling

We used a mathematical model to evaluate how the threshold-stimulus angle affects the minimum distance between predator and prey. This allowed for a consideration of strategy beyond the kinematics of the predator species considered presently. Our analysis was particularly concerned with the minimum distance attained by the predator because that value represents the best opportunity for prey capture. This agent-based model calculated the kinematics of predator and prey with simplified motion. The prey was assumed to be motionless until stimulated to initiate an escape and the predator moved at a constant velocity that was directed toward the initial position of the prey. The first step in such calculations required finding the distance between predator and prey. The visual angle of a predator of width w was calculated from the prey's perspective on the approach with the following relationship:

$$\tan\left(\frac{\theta}{2}\right) = \frac{w}{2d}. \tag{1.2}$$

Solving Eqn. 1.2 where $d = d_{\text{thresh}}$ allowed us to calculate the threshold distance as a function of the threshold visual angle ($\theta = \theta_{\text{thresh}}$). The response distance at the time of the escape was found by considering the reduction due to the prey's latency ($d_{\text{resp}} = d_{\text{thresh}} - ut_{\text{lat}}$, where u is the predator's velocity). The maximum possible value for the threshold visual angle was obtained from Eqn. 1.2 with distance set to the minimum response distance, equal to the

product of predator speed and prey latency:

$$(\theta_{\text{thresh}})_{\max} = 2 \arctan\left(\frac{w}{2ut_{\text{lat}}}\right). \tag{1.3}$$

The minimum distance depends on the kinematics of a prey's escape response. The fast-start allows a fish to attain rapid speeds in a brief period of time. In a preliminary analysis, we varied speed over time, but found that our predictions were similar to an instantaneous onset of the mean escape speed measured in response to the live predator ($v = 3.7\,\text{cm s}^{-1}$, $N = 63$). The fast-start is capable of sending the fish in different directions with respect to the predator, expressed by the escape angle (α). When the predator is slower than the escaping prey, the minimum distance will equal the response distance for low escape angles. These values for minimum distance are expressed by the following equation [76]:

$$d_{\min} = d_{\text{resp}} \text{ if } |\alpha| \leq \arccos(K), \tag{1.4}$$

where K is the ratio of predator to prey speed ($K = u/v$). However, if the predator was faster than the prey, or the escape angle was greater than $\arccos(K)$, we calculated the minimum distance using a previously-developed formulation [76, 91] that assumes fixed velocities for the predator and prey:

$$d_{\min} = \sqrt{\frac{d_{\text{resp}}^2 \sin(\alpha)^2}{K^2 - 2K\cos(\alpha) + 1}}. \tag{1.5}$$

Using Eqns. 1.4 and 1.5, we calculated the minimum distance for when a predator is slower ($K = 0.5$), slightly faster ($K = 1.5$), and much faster ($K = 3.0$) than the prey. At each speed, we examined the effects of 6 values of the escape angle ($0 \leq \alpha \leq 160\,\text{deg}$). In separate calculations, we varied predator speed ($0 < K < 5$) to simulate a visual angle stimulus ($\theta_{\text{thresh}} = 14$ deg). Throughout, small values for the minimum distance ($d_{\min} < 2\,\text{cm}$)

were considered threatening to the prey, based on previous work on the suction feeding of predatory cichlids that are comparable in size to our cichlid predator [87].

1.4 Results

We evaluated the behavioral responses to an artificial stimulus with a novel analytical method. As detailed above, we measured the visual angle prior to an escape response in each experiment. By assuming the latency between the stimulus and response among experiments, we found the response time as the sum of the threshold time and the latency (Fig. 1.2). We examined how our measurements compared to this relationship at variable threshold values for the visual angle (Fig. 1.3A). This analysis considered only experiments where the hypothetical threshold stimulus was attained within a recording prior to the response. Because of this, each value of θ_{thresh} is reported with its corresponding sample size (Fig. 1.3F). As reflected by the coefficient of determination, we found the best matches for a range of threshold values for the visual stimulus ($10.3 < \theta_{\text{thresh}} < 15.8$ deg, $12 < N < 17$, Fig. 1.3D). These threshold values correspond to a range in latency between 740 ms and 780 ms (Fig. 1.3E).

We considered the escape responses of zebrafish to a live predator. Our measurements for the visual angle prior to an escape varied largely due to the relatively rapid movements of the zebrafish (Fig. 1.4A–B). These measurements represent hypothetical threshold cues that stimulated an escape response to the live predator, which we examined for the range of latency values recorded for the projected stimulus (Fig. 1.3E). For each value of the latency, we calculated the first and third quartiles for all measurements of the visual angle. The first quartile was as low as 6.3 deg ($N = 63$) and the third quartile did not exceed 17.4 deg across values of latency (Fig. 1.4C). This quartile range encompassed most of the values measured

in response to the projected stimulus that showed a high coefficient of determination (11.29 deg $< \theta_{\text{thresh}} <$ 15.8 deg).

We used a mathematical model to examine the strategic implications of our measured responses to a looming visual stimulus. As detailed above, our model considered the distance between predator and prey, with particular focus on the minimum distance as the best opportunity for prey capture. In this analysis, minimum distance values of less than 2 cm were considered to offer a high probability of capture in accordance with prior work [87]. This model assumes that the prey remains motionless until initiating an escape, at which point they escape at a fixed velocity (Fig. 1.5A). By also assuming a fixed velocity for the predator, we were able to calculate the minimum distance predicted for a range of threshold values, escape angles, and relative speed of the predator (Eqn. 1.5). In all cases, the minimum distance was predicted to decrease asymptotically toward zero with increases in the threshold-stimulus angle. As a consequence of this non-linear relationship, small differences at the low-end of threshold values were found to have relatively large effects on the minimum distance. As a result, minimum distance values greatly exceeded the proximity at which a suction-feeding predator may typically strike (Fig. 1.5B–D). Within the range of threshold-stimulus angle that we measured, the minimum distance exceeded 2 cm for all but the smallest escape angles if the predator was slower (Fig. 1.5B) or just slightly faster (Fig. 1.5C) than the prey. Our calculations suggest that prey will likely fail to escape the predator at all escape angles if the predator's approach is more than twice as fast as the escaping prey for a predator of width comparable to the cichlid ($w = 2.5$ cm, Fig. 1.5E). Similar results were obtained for a predator that was twice as wide (Fig. S4G), but a substantially more narrow predator would likely succeed in capturing prey at almost all speeds (Fig. S4H).

1.5 Discussion

Our results demonstrate the strategic implications of responses to a looming stimulus by zebrafish. Using a novel analytical method, we found relationships between latency and the threshold-stimulus angle (Fig. 1.3) to an artificial stimulus. We related these results to a live predator (Fig. 1.4) and considered their significance to strategy via mathematical modeling (Fig. 1.5). Our results suggest that zebrafish have a strategic advantage when they respond to the measured threshold-stimulus angle. However, the effectiveness of this response is reduced for relatively fast predators. Our findings offer a strategic basis for understanding the neurophysiology of visual processing and motor commands for the escape responses of fishes.

Our experimental approach addresses a challenge to inferring a sensory cue from behavioral experiments. This challenge emerges from the unknown latency between stimulus and response, which creates ambiguity in the magnitude of the stimulus intensity at the moment the response was stimulated. This latency, which is due to the neurophysiological integration of the visual stimulus and formulation of a motor response, is easily resolved in experiments that consider a discrete stimulus, such as a step-change in light intensity, and an escape response [56, 8]. In contrast, the latency is less clear for a stimulus like the looming appearance of a predator, where the visual angle increases over time. Due to non-linearity in the visual angle of a looming stimulus, small differences in an estimate for latency may yield contrasting values for the threshold-stimulus angle. Our approach determines when a particular threshold-stimulus angle was reached, given the timing of the response and the measurements of the visual angle (Fig. 1.2A). By assuming a consistent latency among all experiments, the response time was presumed equal to the sum of the threshold time and latency. We evaluated how well measurements of response and threshold-stimulus times conformed to this relationship using the coefficient of determination (Fig. 1.2B–C). By that standard, we found that about half of the variation in response time could be predicted

from measurements of the visual angle (Fig. 1.3D). This method yielded a set of values for hypothetical sensory cues and their corresponding latency values, which contrasts the conventional practice of assuming a solitary value for the latency [83, 2, 64, 34].

The present results may be compared to previous studies of similar experimental design. Adult goldfish were found to respond principally to a visual angle of ∼21 deg ($t_{\mathrm{lat}} = 35$ ms) [69], which is roughly half as sensitive as what we observed (Fig. 1.3). The goldfish results are consistent with findings from one study on zebrafish larvae ($\theta_{\mathrm{thresh}} = 21.7$ deg, $t_{\mathrm{lat}} = 35$ ms) [83]. However, another study on larvae found sensitivities that were less than a third of these values ($\theta_{\mathrm{thresh}} \sim 72$ deg, $t_{\mathrm{lat}} = 81$ ms) [27]. Differences in methodology, such as whether the fish were permitted to swim freely and the assumed value for the latency may account for these disparate results. We found a lower threshold for the visual angle in adults (Fig. 1.3) than the studies on larvae, which could be related to differences in predator types between the two groups. A recent study has shown that contrast in addition to visual size is an important parameter that fish use to determine when to escape from a looming stimulus [17].

We considered the implications of the threshold-stimulus angle on the evasion strategy of zebrafish through an application of differential game theory [91, 76]. Our model calculated the minimum distance attained between the predator and prey, assuming a fixed velocity for both fish (Fig. 1.5A). Reductions in the visual angle (Fig. 1.5B–D) show disproportionate increases in the minimum distance, due to their nonlinear relationship. Our experiments suggest that zebrafish respond to visual angles where they are predicted to successfully evade predators, provided the predator is relatively slow (Fig. 1.5B–C). However, the prospects for survival declined precipitously if the predator approached the prey at more than twice the escape speed (Fig. 1.5E). This supports our hypothesis that zebrafish escape from a threshold visual angle that allows them to remain at a safe distance from an approaching predator. By varying the size of the predator, we found that narrower predators had an

advantage over wider predators (Fig. S4), because the narrower predator can approach a closer distance to the prey before the threshold-visual angle is detected by the prey.

The result of a prey's evasion strategy depends on the actions of the predator. Although predator fish are generally capable of faster swimming than prey, it is common for suction-feeding predators, such as the cichlid considered presently, to approach their prey slowly. Many species actively brake on the approach by expanding their pectoral fins [40, 41]. Suction feeding offers a brief and spatially-limited opportunity to capture prey [20, 45] and it could be that braking enhances the precision of a strike. By contrast, the fast-start is the most rapid swimming of which a fish is capable and may therefore routinely exceed the speed of a suction-feeding predator [77, 80]. Therefore, slow predators may be common in many predator-prey encounters. Relying on the visual angle to stimulate an escape may therefore be successful for prey like zebrafish when they encounter a variety of suction-feeding fish predators.

In summary, we found responses to the visual angle from behavioral responses of zebrafish adults to a projected looming stimulus and live predator. By modeling the kinematics of predator and prey, we considered how these responses affect the evasion strategy of zebrafish. These calculations illustrate how the visual angle provides a robust sensory cue for escaping predators at sufficient distance for a high probability of survival. However, our results also demonstrate the limits to the measured threshold-stimulus angle, which generally fails when the predator is more than twice as fast as the prey (Fig. 1.5E). This combination of experimentation and mathematical modeling has the potential to reveal how sensory cues affect the strategy of both predator and prey in a diversity of animals.

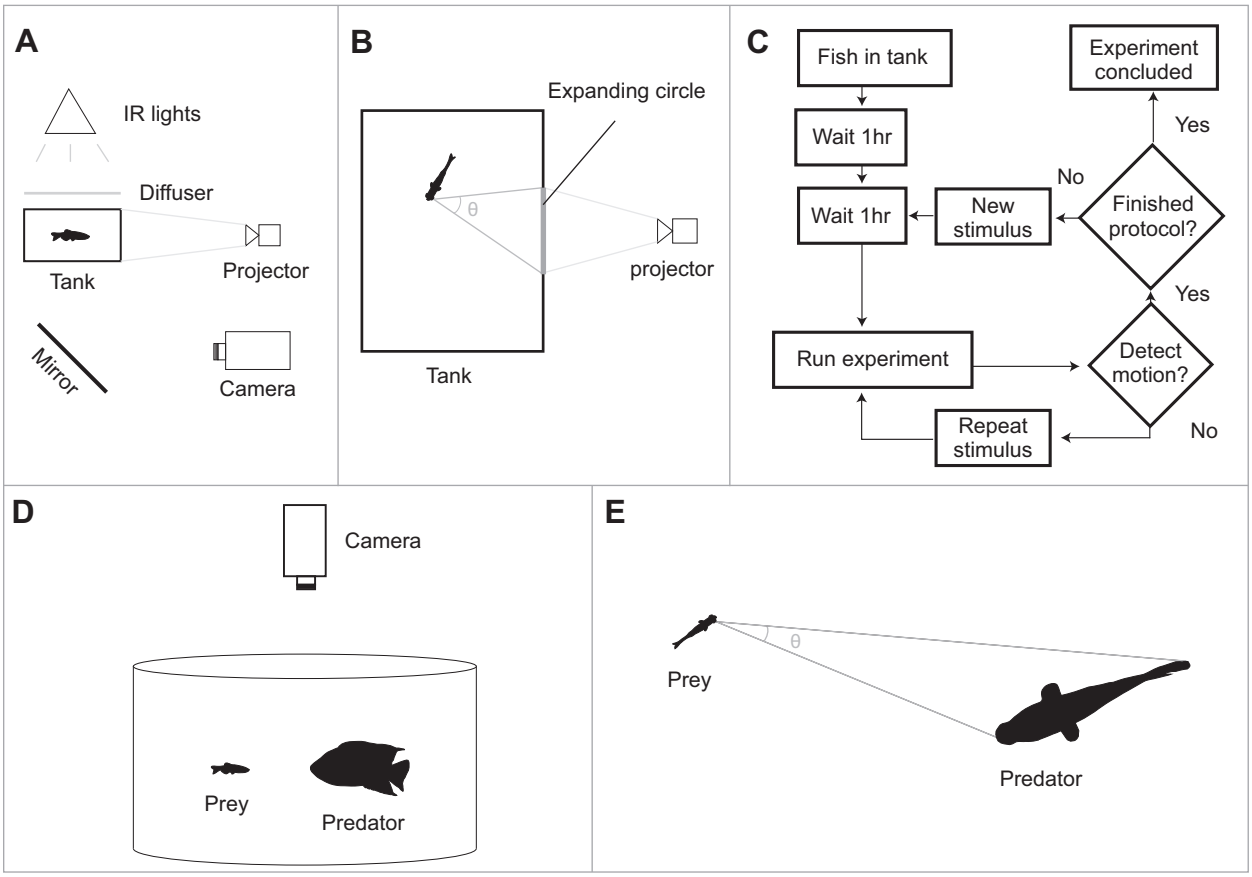

Figure 1.1: Experimental methods using an artificial and live looming stimulus. (A) In the artificial stimulus setup, a camera viewed the underside of the fish in the tank using a mirror at a 45 deg angle. The stimulus, a circle of expanding diameter, was projected on the side of the tank by a projector. (B) As seen from below, the stimulus presented a visual angle (θ). (C) Flow chart for the sequence of automated experiments using the artificial stimulus. Computers controlled the timing of the experiments. (D) In experiments with a live predator, an individual zebrafish was introduced into a large circular tank with a red Texas cichlid. (E) The visual angle was measured from the eye of the prey to the margins of the predator's body.

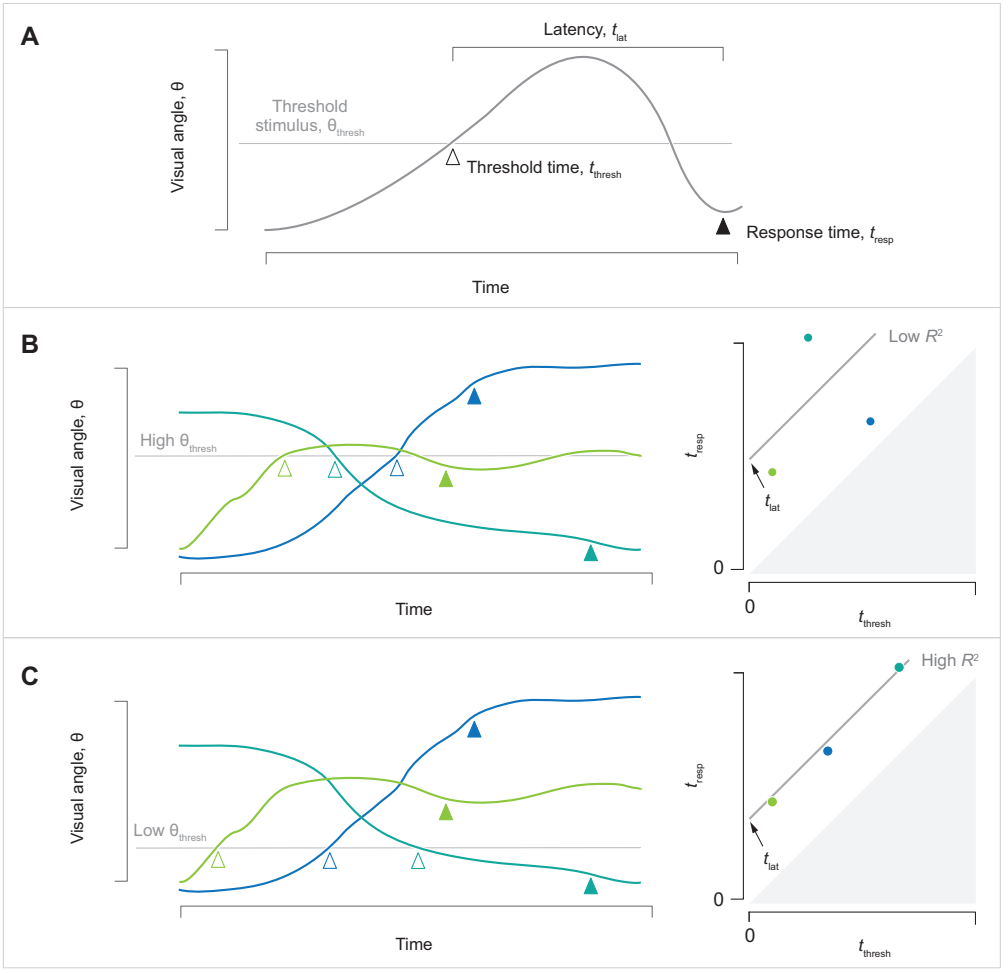

Figure 1.2: Analytical method for testing values for the threshold-stimulus angle. (A) Measurement of the visual angle for a hypothetical experiment with annotations for the response time (t_{resp}, filled triangle) and threshold time (t_{thresh}, open triangle), when the threshold angle was exceeded. The threshold time was estimated by assuming a particular value for the threshold visual angle (θ_{thresh}) and the latency (t_{lat}) was determined as the difference between stimulus and response times. (B–C) The same three experiments (denoted by the colored lines) were analyzed assuming a high (B) and low (C) threshold stimulus, given measured values for the visual angle and response time (denoted by filled triangles, left plots). The first time the visual angle exceeds the threshold-stimulus angle is the threshold time (denoted by empty triangles, left plots). As detailed in the text, the relationship between the stimulus and response times (right plots) should conform to a linear relationship with a slope of unity and a y-intercept equal to the latency. In this example, a better fit to this relationship was obtained by assuming a low threshold (C) than a high threshold (B), as would be indicated by the coefficient of determination (R^2, right plots).

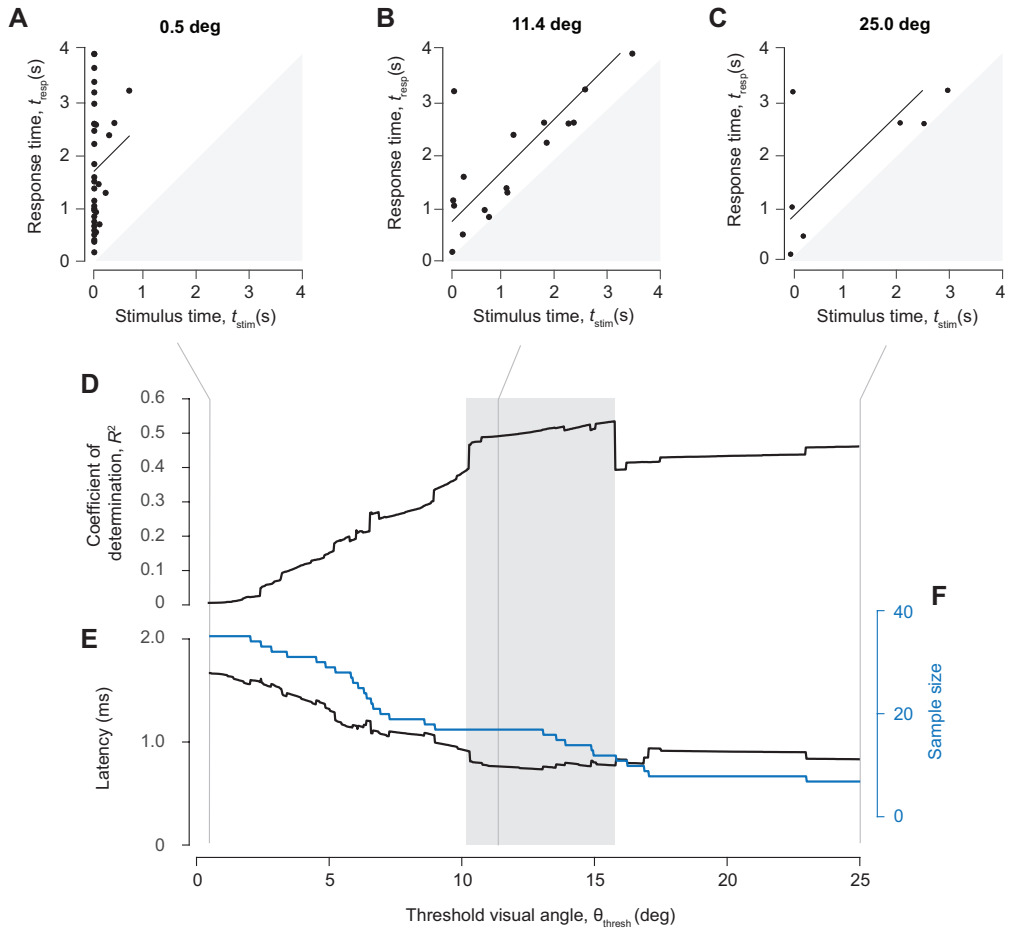

Figure 1.3: Determination of the threshold visual angle for all experimental responses to a projected looming stimulus. (A–C) Relationship between the threshold and response times for three representative values for the threshold visual angle. As described above (Fig. 1.2), this relationship is predicted to conform to a slope of unity, with a y-intercept equal to the latency predicted for each value of the threshold-stimulus angle . (D) The coefficient of determination for the unity-line fit for each value of the threshold-stimulus angle , (E) the corresponding latency, and (F) sample size (blue) are plotted . Experiments with an escape occurring before the threshold-visual angle was seen were removed, resulting in a decreasing sample size as threshold-visual angle increases. We selected values for latency and the threshold visual angle where the coefficient of determination was relatively high (gray bar) for comparison with responses to a live predator (Fig. 1.4).

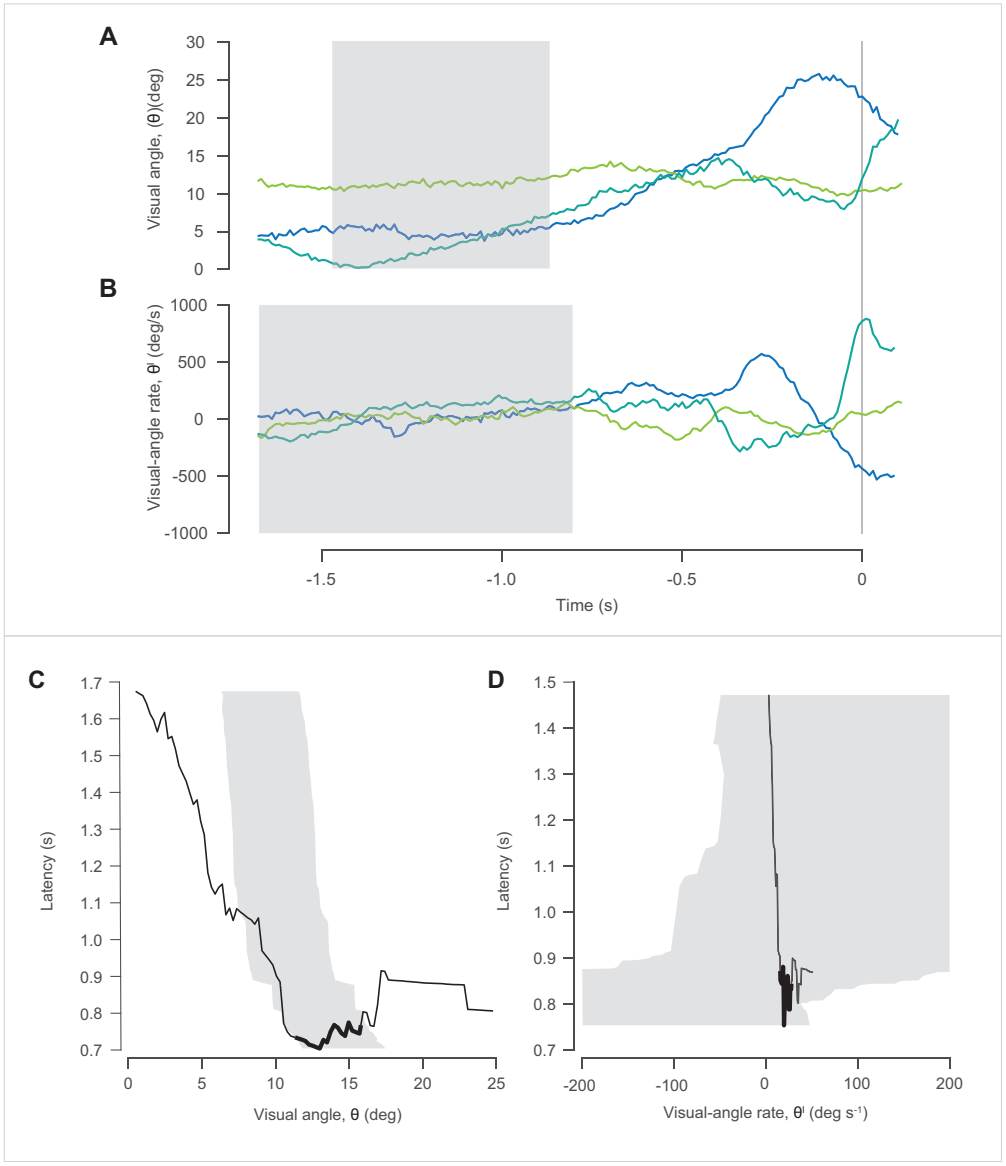

Figure 1.4: Responses to a live predator. (A and B) Three representative measurements of the visual angle (colored lines) , with time calculated relative to the response time (gray line). We considered all values for the range of latency values (gray bars) suggested by measured responses to a projected stimulus (Fig. 1.3). (C and D) Comparison of measurements from the projected-stimulus experiments (black curves) and live-predator experiments (gray areas) for the threshold-stimulus angle . The margins for the live predator are the first and third quartiles of values for the threshold-stimulus angle at each value for the latency. The regions of the threshold-stimulus angle with a high coefficient of determination (gray bars in Fig. 1.3) which fall within the bounds of the live-predator experiments are highlighted (heavy black curves).

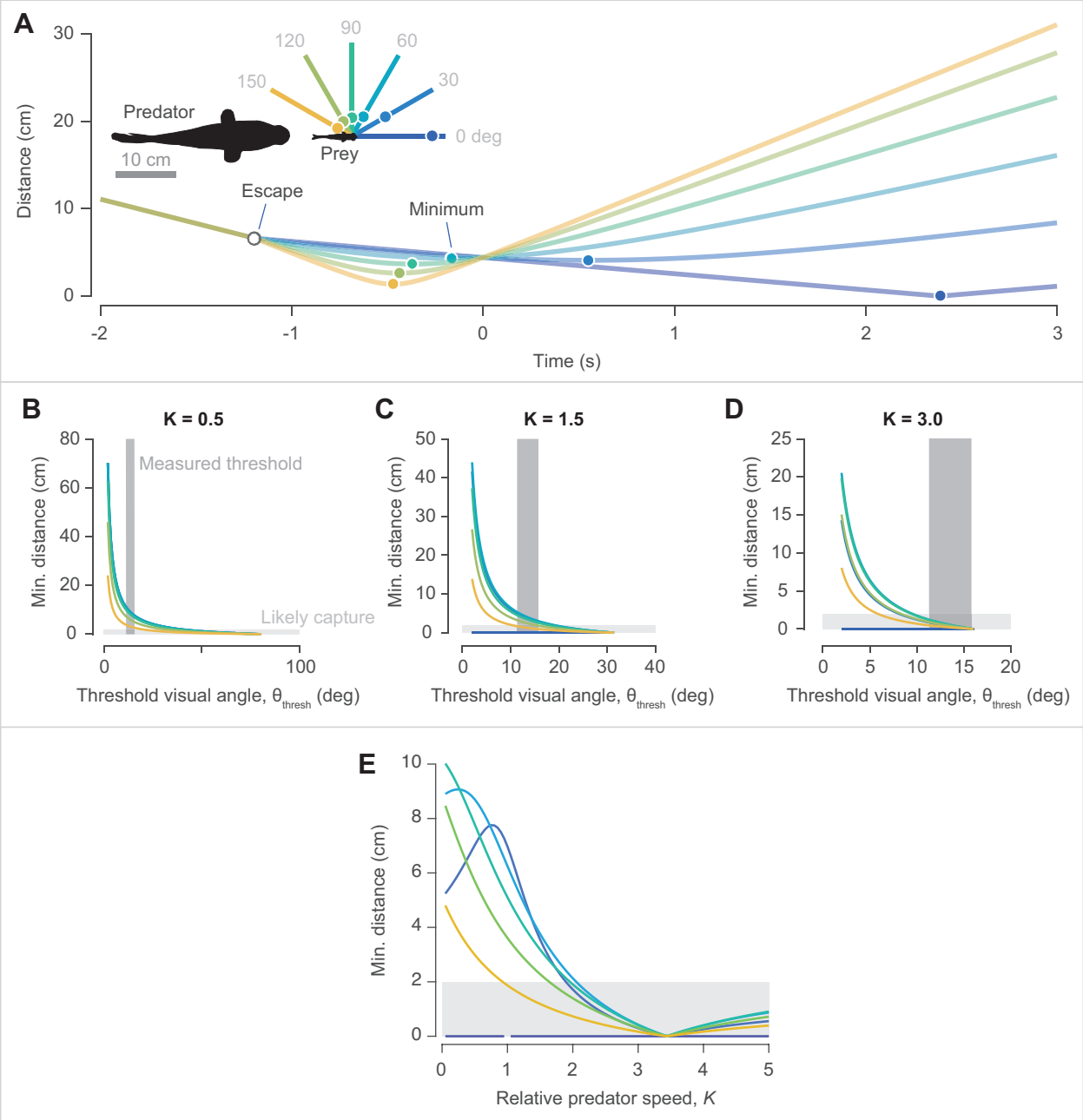

Figure 1.5: (legend next page)

Figure 1.5: The effects of the threshold-stimulus angle on the evasion strategy of zebrafish. (A) Numerical simulations of kinematics of predator and prey shows the distance between the predator's rostrum and prey's center of body over time for escape directions between 0 and 150 deg where relative predator speed (K) = 1.5, the latency time (t_{lat}) = 0.8 s, the threshold angle (θ_{thresh}) = 10 deg, predator size (S) = 2.5 cm, and prey velocity (V) = 3.7 cm s^{-1}. Time = 0s is when collision between predator and prey would have occurred if escape had not been initiated. The inset shows the relative position of predator and prey at the start of the escape and the radiating lines show the prey's trajectory for differing escape direction with the same color coding as all other panels. The minimum distance occurs at the position of the filled circles in both the graph and insert. (B–G) The minimum distance predicted (Eqn. 1.5) for varying threshold values for the visual angle (B–D) and its rate (E–G). The vertical bars (dark gray) indicate the range of threshold values favored by our analysis of experiments (Fig. 1.4). The horizontal bars (light gray) indicate distance values where the prey have a low probability of escape ($d_{\mathrm{min}} < 2$ cm). Calculations were performed for predators of variable relative speed ($K = 0.5$, $K = 1.5$, and $K = 3.0$). (E) The minimum distance as a function of relative predator speed at particular values of the threshold visual angle ($\theta_{\mathrm{thresh}} = 14$ deg).

Chapter 2

Fish use their vestibular system and lateral line to respond to impulsive flows.

2.1 Abstract

Fish have many senses useful for evading predation. In this study, we examined two: lateral line and the vestibular system. The lateral line detects water flows adjacent to prey fish and the vestibular system detects the acceleration of the prey's body and its orientation with respect to gravity. It is unclear how useful these senses are in evading predators. Water flows that indicate an approaching predator may be detected by the lateral line or, if it is strong enough to accelerate the prey fish, by the vestibular system. We examined how different parts of the lateral line, the superficial and canal neuromasts, differentially help fish detect impulsive flows which may be indicative of danger. We also examined whether the vestibular system can be used to detect these impulsive flows indirectly, by means of accelerating the

body. Through chemical ablation of the lateral line or only the superficial neuromasts and exposing fish to a series of impulsive flows in the dark, we show that fish are more likely to escape from an impulsive flow if they have use of their full lateral line. However, even fish with no functioning lateral line are capable of responding to an impulsive flow, indicating that the vestibular system is sufficient to detect these flows. This study lends new evidence to show that multiple senses are capable of responding to the same flow stimulus.

2.2 Introduction

Sensing an approaching predator is essential for fish to evade predation. Flow sensing allows fish to detect the bow wave generated by an oncoming predator [79]. Previous studies have explored the effects of flow sensing by the lateral line on predator evasion [78, 12, 57]. A previous study [11] showed that CNs allows zebrafish to forage for food from a larger distance away than SNs alone. However, this difference has not been examined in depth with respect to predator avoidance. Additionally, the vestibular system, which detects the acceleration of the body of fish, may serve as an indirect sensor if the flow propels the fish. However, this ability has not been studied in the context of predator avoidance. In this study, we investigate the ways prey fish use their SNs, CNs, and their vestibular system to respond to flow that may indicate an approaching predator.

Fish sense water flow with their lateral line, which extends from their head down the length of the body [22]. The lateral line includes neuromasts which are flow receptors that include hair cells arranged in clusters and covered with a gelatinous cupula. As water passes over a neuromast, the cupula and the underlying hair cells are deflected, causing the affliated lateral line neuron to change the frequency of its action potentials [22]. The lateral line of fish include two types of neuromasts. Large, imbedded canal neuromasts (CNs) detect pressure differences along the fish's body that correlate with the acceleration of flow with

respect to the fish's body [22, 89]. Smaller superficial neuromasts (SNs) are attached to the surface of the fish's body and detect the velocity of water with respect to the fish's body [22, 89]. In this study, we used short-duration flows, or impulsive flows, as a proxy for the flows created by an approaching predator. Preliminary experiments established that zebrafish initiated escape responses when exposed to impulsive flows (personal observation, Amberle McKee). These impulsive flows offer a change in acceleration and velocity which should trigger both the CNs and the SNs, respectively.

We hypothesized that CNs and SNs work together to produce a stronger signal in fish than the CNs can provide alone. We therefore tested whether there was a difference in a fish's ability to detect impulsive flows when they had either their SNs compromised or the entire lateral line compromised. We exposed fish to varying levels of the antibiotic neomycin sulfate, which is known to ablate hair cells [12]. This technique produced three groups of fish: those with their lateral line intact (CN+SN), those with their SNs temporarily ablated (CNs-only), and those with both their CNs and their SNs temporarily ablated (no-LL). We exposed each group to impulive flow in the dark and compared their startle reactions. We predicted that CNs-only fish would be able to detect impulsive flows better than no-LL fish and that CN+SN fish would be able to detect impulsive flows better than either of the other two groups of fish.

The vestibular system in the fish's inner ear allows fish to detect the acceleration of its body, including the acceleration of gravity which provides information on the fish's orientation [37]. This system also contains hair cells that work in a similar way to the lateral line hair cells. When the body of the fish is accelerated, fluid in the semicircular canals in the inner ear and otoliths accelerate at slightly different rates, deflecting the cupulas of hair cells in the inner ear [81] to transduce the fish's linear and rotational acceleration [81].

A previous study [78] showed that the specific gravity of zebrafish larvae (which is determined by how inflated the swim bladder is) determines how much the fish's body moves with the

surrounding fluid during a suction feeding event. In another study [42] researchers showed that the turbulence of the water affects prey fish's ability to sense predators in the same way. This relative movement of the fish's body with respect to the water affects the information provided to both the lateral line and the vestibular system. If the fish's body is moving at the same rate as the water, the lateral line will not be stimulated, but the vestibular system will if the body is accelerating. Conversely, if the fish's body does not move when water flows around it, the lateral line will be stimulated but the vestibular system will not. Prey fish can acclimate to a flow stimulus, however, and adapt their predator detection accordingly [33]. These studies motivated us to examine whether a vestibular stimulus alone was sufficient to trigger a C-start in fish.

We hypothesized that if a flow is accelerated to a sufficiently high velocity, the flow may accelerate the body of the fish, triggering the vestibular system in addition to the lateral line system. To test this hypothesis, we temporarily ablated experimental fish's lateral line (no-LL) and then exposed them to an impulsive flow in the dark and monitored their reaction. This allowed us to isolate the input to the vestibular system. We predicted that at low flow speeds, fish would be unable to detect the flow with their vestibular system only because the slow speed of the water would be unable to accelerate the fish's body. However, at high flow speeds, we predicted that fish's body would be accelerated and the fish would show a reaction, even with their lateral lines and vision compromised.

To test these predictions, we created and used a larger version of the impulse chamber from this study [57]. This chamber allows a short-duration, controlled, repeatable, impulsive flow to be created in a tank of water containing a free-swimming fish. We used this chamber to expose fish to impulsive flows of different velocities. We treated some of the experimental fish with a neomycin sulfate solution to ablate either part or the entirety of their lateral line. With these treatments and the impulse chamber, we were able to investigate the role of the lateral line and vestibular system on escape responses in zebrafish.

2.3 Methods

2.3.1 Animal husbandry

Wild type (AB line) zebrafish, were raised according to standard procedures. The fish were held in a flow-through tank system (Aquatic Habitats, Apopka, FL, USA) in 3 L containers at 27°C and fed daily and with a 14:10 h light:dark cycle. All rearing and experimental protocols were conducted with the approval of the Institutional Animal Care and Use Committee at the University of California, Irvine (Protocol #AUP-17-012).

2.3.2 Setup

An impulse chamber was used to run experiments on adult fish in a repeatable, impulsive flow (Fig. 2.1A). The large, rectangular tank (91.44 cm x 73.66 cm) was divided by two sheets of acrylic (0.64 cm thick) with many mesh windows throughout to allow the flow of water. Two smaller plates of acrylic (0.64 cm thick) stood at right angles to the larger two sheets with mesh. These four acrylic plates created the walls of the inner tank (37.47 cm x 9.52 cm) where fish were kept during experiments, called the working section following. Attached to one of the larger acrylic plates was an acrylic tube (3.81 cm inner diameter; 34.29 cm long) with mesh covering the end of the tube that was attached to the working section so water could flow between the tube and the working section, but fish could not pass between them. Inside the tube, a specialized piston fit snugly to create flow within the working section when moved within the tube. The piston was specially-designed with grooves that minimized any sound when the piston moved within the tunnel.

A linear servo motor (LinMot PS01-37X12OF-HP-C, Spreitenbach, Switzerland) above the tank, attached to the piston via another thin acrylic plate. When the motor moved forward

or backward, the piston moved accordingly within the tube. During the experiments, the piston was pulled backwards by the motor at a specified velocity and acceleration (detailed in the next section) to create the desired flow over the working section of the impulse chamber (Fig. 2.1B). The motor was moved by a controller (LinMot Type:E1100-GP, Spreitenbach, Switzerland), which was controlled with software (LinMotTalk 6.6 Build 20170704, Spreitenbach, Switzerland). A high-speed video camera (FastCam Mini UX50 type 160-M-16G, Photron, San Diego, CA) positioned above the tank allowed a detailed view of the working section and the fish within it. The camera was controlled with software (Photron FastCam Viewer Version 3670, San Diego, CA) and triggered by the motor. Around the tank, infrared (IR) lamps (IR Illuminator CM-IR200, Houston, Tx, USA) provided light to the camera that the fish could not see.

2.3.3 Experiments

We used three treatment groups of fish (SNs + CNs, no-LL, and CNs-only) which were each exposed to four flow speeds (0.35 cm/s, 0.55 cm/s, 0.69 cm/s, and 2.76 cm/s) and one control (the camera recorded but the motor was not activated). Each fish was allowed to acclimate in the working section of the impulse chamber for 2 hrs in the dark, individually. The researcher then entered the room and waited an additional 15 min before starting the experiment to avoid any effects of the door closing or the researcher moving around. After this period, the researcher would trigger a motor controller using the motor-control software. The controller would trigger the motor to pull the piston back at the specified velocity and the camera to record the fish in the working section at the same time (camera recorded at 1000fps 896x264 resolution). After each trial, the camera saved the video and the researcher reset the piston and prepared for the next trial. This procedure repeated until the fish had been exposed to each of the four flow speeds and a control trial in a randomized order with

15 min breaks between the end of the piston reset and the beginning of the next trial. The lights remained off for the duration of the experiment to prevent the fish from using vision.

Each fish was assigned to one of three treatment groups: SNs + CNs, no-LL, and CNs-only (Fig. fig:methodsC-E). Fish in the SNs + CNs group were untreated before entering the impulse chamber. Fish in the no-LL group was treated with 0.12 g of neomycin sulfate that was dissolved in a 100 mL volume of water buffered with 1 mL of bicarbonate solution (1.68 g $NaHCO_3$ / 20 mL water) for 2 hrs to temporarily ablate the entire lateral line system. After ablation, these fish were rinsed by changing their fresh water three times at 5 min intervals. They were then allowed to recover for a minimum of 15 min before being moved to the impulse chamber. Fish in the CNs-only group were first anesthetized with a dilute MS-222 solution (0.4 g MS-222 dissolved into 100 mL water and buffered with Tris base until pH = 7. 16.8 mL of this concentrated MS-222 solution is this diluted into 100 mL water). A concentrated paste of neomycin and agar (2 mL neomycin concentrate [2 g neomycin dissolved in 10 mL water] and 2 mL 4 percent agar solution) was brushed onto both sides of the body with a paintbrush and allowed to remain for 10 s before being wiped away with a paper towel. The fish was then immediately moved to fresh water and rinsed, as above. These fish were exposed to overhead lighting for a minimum of 15 min before being moved to the impulse chamber, which further ensured that the neomycin stopped ablating more of the lateral line. This procedure resulted in fish with diminished superficial neuromasts and intact canal neuromasts.

This procedure was tested on non-experimental zebrafish prior to its use on experimental fish. This preliminary testing showed that fish behaviorally recovered from the procedure. Additionally, the effectiveness of the treatment to ablating lateral line neuromasts was determined with a flourescent vital stain for hair cells (DASPEI, 2-(4-(dumethylamino)styryl)-N-ethylpyridinium iodide, Fig. 2.1).

2.3.4 Statistical Analyses

Each video was manually-scored to decide if and when an escape, in the form of a C-start, was initiated. A behavior was defined as an escape when the fish curled into a 'C' shape within 10 ms and accelerated as they uncurled. This data was then analyzed with statistical software (MATLAB, version R21015a, Mathworks, Natick, MA, USA). A logistic regression was used to determine if there was a difference in whether or not fish escaped between the three treatment groups and the five trials (four flow velocities and one control). A series of Bonferoni-corrected ANOVAs were used to determine if there was a difference in the time from the start of the trial to the initiation of a C-start between each treatment group within each velocity.

2.4 Results

The fish's reaction to flow stimuli was analyzed across all trials and treatment groups. Among the 20 fish in each treatment group, 27 showed a C-start response during the course of the experiment in the SNs+CNs group, 9 in the no-LL group, and 12 in the CNs-only group. Among those, only one fish showed a C-start response during a control experiment (i.e. no flow stimulus). Since this fish was in the no-LL group, there was no flow, and the C-start was initiated very late in the course of the experiment, this data point was removed as an outlier during subsequent analyses. We analyzed the probability of escape (Fig. 2.2A) and the time between the onset of flow to the beginning of an escape (Fig. 2.2B) between each velocity and across treatment groups.

We found that many of the escape responses occurred while the piston was moving, and many occurred well after the piston stopped (Figs. 2.3 and 2.4). The latter group may be a delayed response or a reaction to something else we cannot foresee. Therefore, we elected to

analyze the data in two ways: once with all of the data, and once discounting the C-starts that occurred after the piston movement stopped. The first set of analyses provided includes the data from every fish and trial.

A logistic regression showed a difference in escape probability between different treatment groups, but no difference in escape probability across different flow velocities. This regression predicted the escape probability at flow velocity 0.69 cm/s is 10 orders of magnitude lower than the escape probability at 2.76 cm/s ($p = 1.00$, $n = 47$). Similarly, the regression predicted the escape probability at flow velocity 0.55 cm/s is 50.6% the escape probability at 0.69 cm/s ($p = 0.13$, $n = 47$), the escape probability at flow velocity 0.35 cm/s is 63.2% the escape probability at 0.55 cm/s ($p = 0.29$, $n = 47$), and the escape probability at flow velocity 0 cm/s is 44.6% the escape probability at 0.35 cm/s ($p = 0.08$, $n = 47$). The regression also predicted the escape probability for CNs-only is 26.7% of the escape probability for CNs+SNs ($p < 0.01$, $n = 47$). The escape probability for no-LL is 99.2% of the escape probability for CNs-only ($p < 0.01$, $n = 47$). The regression also showed a small but significant effect of fish identity (104%, $p < 0.01$, $n = 47$). These results suggest that predator detection is enhanced with the number of sensory systems available.

An ANCOVA was performed to examine the statistical difference in the time to escape between the three treatment groups with flow velocity as a covariate. We found that there was a small, significant difference between lateral line treatment groups ($F = 3.7$, $df = 2$, $p = 0.03$, $n = 47$). A Tukey-Kramer test was performed to determine which particular groups differed. This test indicated that the fish with no lateral line were significantly different from the fish with their lateral line intact ($p = 0.03$, $n = 47$). These results suggest that the timing of escape initiation is affected by the complete lateral line.

The following reports the results of re-analyzing the data without the trials where an escape occurred after cessation of piston motion. As stated earlier, this was done to take into account any unaccounted-for reason as to why fish initiated an escape after the piston finished moving.

There were 35 total fish that initiated an escape in this analysis. Of these, 5 were no-LL, 7 were CNs-only, and 23 were CNs+SNs.

A logistic regression showed a significant difference in escape probability between treatment groups and no difference between flow velocities. This regression predicted the escape probability at flow velocity 0.69 cm/s is 10 orders of magnitude lower than the escape probability at 2.76 cm/s ($p = 1$, $n = 35$). Similarly, the regression predicted the escape probability at flow velocity 0.55 cm/s is 78.2% the escape probability at 0.69 cm/s ($p = 0.61$, $n = 35$), the escape probability at flow velocity 0.35 cm/s is 57% the escape probability at 0.55 cm/s ($p = 0.29$, $n = 35$), and the escape probability at flow velocity 0 cm/s is 53.7% the escape probability at 0.35 cm/s ($p = 0.24$, $n = 35$). The regression also predicted the escape probability for CNs-only is 17.6% of the escape probability for CNs+SNs ($p < 0.01$, $n = 35$). The escape probability for no-LL is 25.2% of the escape probability for CNs-only ($p < 0.01$, $n = 35$). The regression also showed a small but significant effect of fish identity (104%, $p < 0.01$, $n = 35$). These results suggest that predator detection is enhanced with the number of sensory systems available, in agreement with the results of the previous analyses on the entire dataset.

An ANCOVA was performed to examine the statistical difference in the time to escape between the three treatment groups with flow velocity as a covariate. We found that there was no significant difference between lateral line treatment groups ($F = 2.12$, $df = 2$, $p = 0.14$, $n = 35$). These results suggest that the timing of escape initiation is not affected by the lateral line, in contrast to the results of the ANCOVA on the enitre dataset.

2.5 Discussion

Fish have two different sets of hair cell-based sensory systems that may be useful in detecting approaching predator the vestibular system and the lateral line system. The lateral line system, composed of canal nueromasts and superficial neuromasts [22, 89], allow fish to detect water flows around its body. The vestibular system detects body's acceleration and its orientation with respect to gravity [1, 37]. In this study, we examined the effectiveness of the vestibular system and each part of the lateral line system to detect impulsive flows that may indicate an approaching predator.

Through progressive ablation of the lateral line systems, we found that ablation of the lateral line affects the probability of escape from an impulsive flow, but not the timing. When fish had no lateral line, they were still able to escape from the flow stimulus, indicating that they were likely able to detect the impulsive flow with their vestibular system. However the probability of escape in this group was low suggesting that although the vestibular system is sufficient to initiate an escape response, it may not be a reliable cue for predator evasion without the input of other senses. The escape probability significanly increased when they retained their canal neuromasts and increased further when they retained their entire lateral line. This demonstrates the unsurprising fact that having more senses available to the fish increases their ability to detect an impulsive flow stimulus and react to it.

A group of cells in the hindbrain of fish and amphibians called the Mauthner cells largely determine whether a fish initiates an escape from a stimulus [31, 54]. Inputs from the lateral line integrate in the Mauthner cells with inputs from vision and other sensory systems [53]. Auditory and vestibular escapes are also mediated by the Mauthner cell in zebrafish [52, 21, 62, 29]. Once these cells reach a threshold, an escape is initiated. Input from the vestibular system to integrating in the Mauthner cell may increase the probability of an escape based on a flow stimulus. The vestibular system's ability to initiate an escape on its

own may make up for other senses if they are lost. Alternatively, the vestibular system's ability to initiate an escape may compliment the other senses to detect when a stimulus is truly a threat. The same may be true of the effect of different lateral line neuromast types. An adult fish may lose access to one of the two types of neuromasts in a natural setting and need to rely solely on the other. Alternatively, given that the two types detect different information about a stimulus, their combined input may increase the probability of escaping a threatening predator.

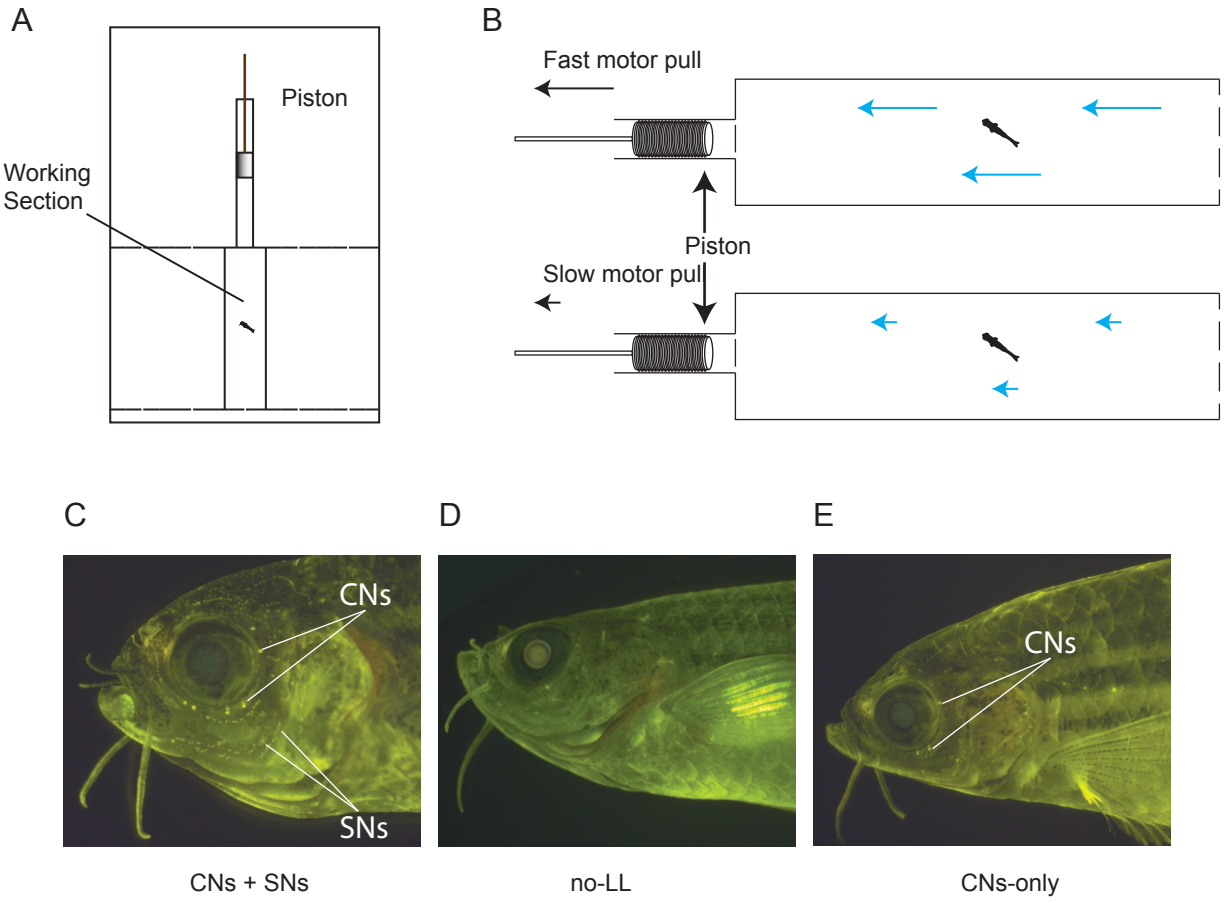

Figure 2.1: Schematic of impulse chamber and how it works. A) In this overhead schematic of the impulse chamber tank, the dashed lines indicate where mesh was substituted to solid wall in order to facilitate the passage of water. The experimental fish was kept in the working section. A motor pulled back on the rod (brown) attached to the piston creating a negative pressure in the tube connected to the working section. This caused water to flow through the working section into the tube, creating a flow over the fish. B) When the motor pulled the piston quickly, it resulted in a faster flow through the working section than when the motor pulled the piston slowly.

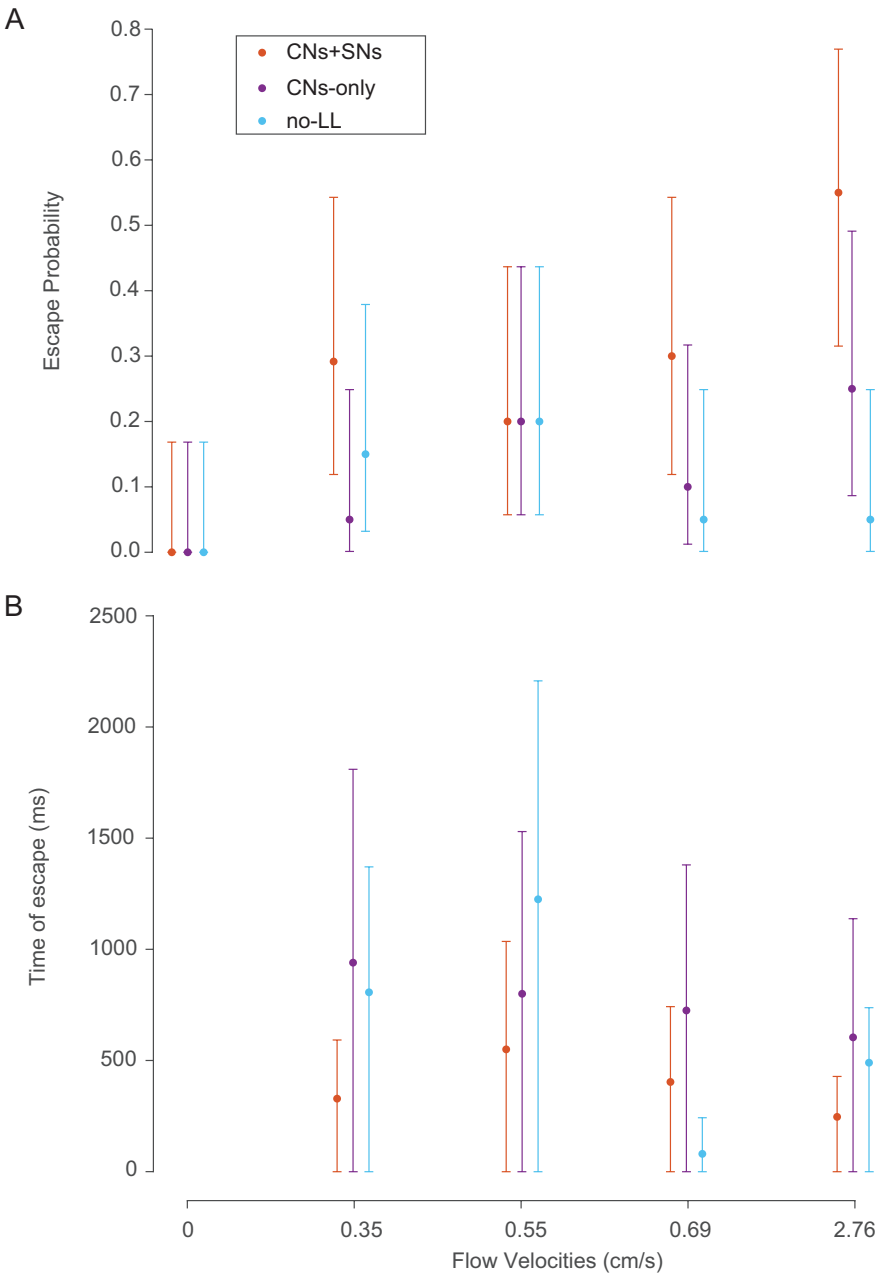

Figure 2.2: A. This is a boxplot with all of the data showing the escape probability and the 95 percent confidence intervals at each of the flow velocities and within each treatment group. A logistic regression showed differences between treatment groups, but not between flow velocities (see Results for details). B. This is a boxplot with all of the data showing the mean time from the beginning of the stimulus to the initiation of an escape response and the 95 percent confidence intervals around them at each of the flow velocities and within each treatment group. An ANCOVA did not find strong differences between groups (see Results for details).

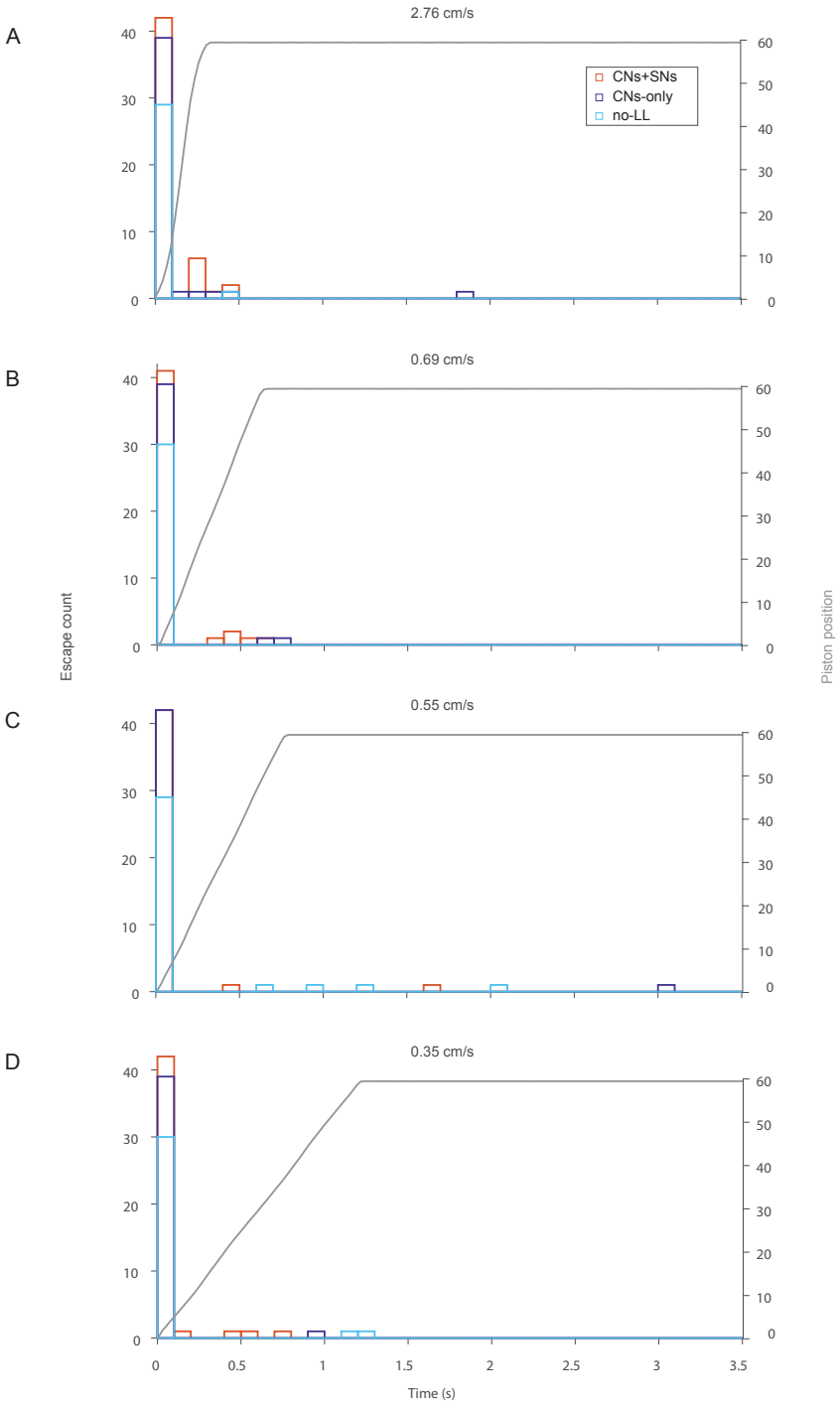

Figure 2.3: The black line on each graph shows the position of the motor and piston over time relative to their starting position. The larger numbers on the y-axis indicate the piston is farther from the working section. Each vertical line indicates that a fish initiated an escape response at that time. The red lines indicate an SNs + CNs fish initiated an escape response, the blue indicate a no LL fish did the same, and the green indicates a CNs only fish.

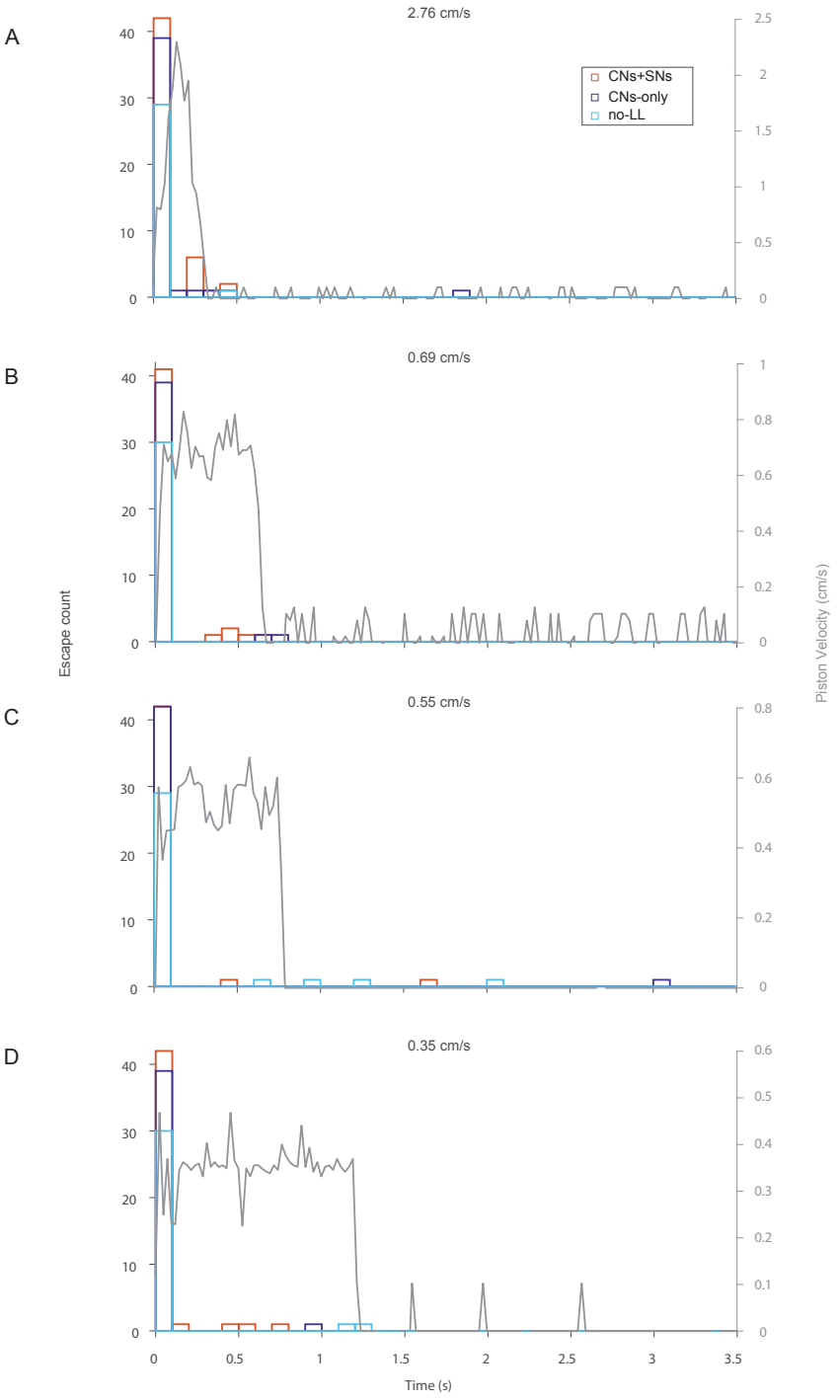

Figure 2.4: The black line on each graph shows the velocity of the motor and piston over time relative to their starting position. Each vertical line indicates that a fish initiated an escape response at that time. The red lines indicate an SNs + CNs fish initiated an escape response, the blue indicate a no LL fish did the same, and the green indicates a CNs only fish.

Chapter 3

The sensory basis of schooling by intermittent swimming in the rummy-nose tetra (*Hemigrammus rhodostomus*)

3.1 Abstract

Schooling is a collective behavior that enhances the ability of a fish to sense and respond to its surroundings. Although schooling is essential to the biology of a diversity of fishes, it is generally unclear how this behavior is coordinated by different sensory modalities. We used experimental manipulation and kinematic measurements to test the role of vision and flow sensing in the rummy-nose tetra (*Hemigrammus rhodostomus*), which swims with intermittent phases of bursts and coasts. Groups of five fish required a minimum level of illuminance (> 1.5 lx) to achieve the necessary close nearest-neighbor distance and high polarization for

schooling. Compromising the lateral line system with an antibiotic treatment caused tetras to swim with greater nearest-neighbor distance and lower polarization. Therefore, vision is both necessary and sufficient for schooling in *H. rhodostomus* and both sensory modalities aid in attraction. These results can serve as a basis for understanding the individual roles of sensory modalities in schooling for some fish species.

3.2 Introduction

Schooling is essential to the biology of a diversity of fish species. A school provides a fish with the potential to enhance their ability to identify prey, detect predators, and swim efficiently [19, 5, 36] by responding to the motion of neighboring fish [51, 4, 50]. Despite this importance, it remains largely unclear how different sensory modalities facilitate communication and decision-making among the individuals in a school. Therefore, the aim of the present study was to test the roles of vision and the lateral-line system in schooling by the rummy-nose tetra (*Hemigrammus rhodostomus*; Ahl, 1924).

Vision and flow sensing are the two sensory modalities thought to facilitate schooling. Pitcher and Partridge tested the roles of these sensory systems in a pelagic marine species, the pollock (*Pollachius virens*) [68, 65]. They found that blinded pollock were capable of schooling, but only with a functional trunk lateral line, which supports the notion that both modalities are sufficient for the behavior. Flow sensing may also be sufficient for shoaling in blind cavefish [84, 49], but a number of fish species are incapable of schooling in the dark [74, 46, 85, 3]. The inability to school in darkness indicates that flow sensing is insufficient and that vision is necessary and likely sufficient. Therefore, the extent that schooling depends on vision or flow sensing varies among fish species.

Vision and flow sensing may play distinct roles in the social behavior of fishes. Shoaling is a general category of behaviors that cause fish to congregate because they are attracted to one-another. In close proximity, fish are commonly repelled by other individuals, which serves to minimize collisions [7]. Schooling is a form of shoaling where the fish move with a similar heading [67], measured as the group polarization. The polarization of a group may be achieved indirectly as a consequence of fish moving toward other fish [51], or results from actively seeking alignment with neighbors [35, 94]. Pollock swim more closely together when the lateral line system is compromised, which supports the hypothesis that flow sensing mediates repulsion and vision is the modality used for attraction [65]. This modality-partitioning is compatible with the spatial limitations of the lateral line system [58] and the visual system's capacity for attraction toward fish at a distance [14]. However, disrupting the lateral line in other species causes the distance between individuals to increase [30, 59], which suggests that flow sensing can aid in attraction, unlike what was has been reported in some other species [67, 9].

The present study evaluated the sensory basis of schooling in a tetra species that swims intermittently with alternating phases of bursts and coasts [10, 55]. These distinct locomotor phases may be analyzed discretely and have the potential to yield contrasting collective behavior from species that move continuously [38]. We measured the swimming kinematics of groups of *H. rhodostomus* individuals both over long durations and with high-speed video in separate experiments. The role of vision was considered by manipulating the illuminance of visible light. The effects of flow sensing were tested by exposure of the lateral line to an aminoglycoside antibiotic, which causes cell death and otherwise attenuates mechanotransduction by lateral line hair cells [39, 86].

3.3 Materials and methods

We video-recorded the swimming of groups of 5 rummy-nose tetra (*H. rhodostomus*, 2.48 ± 0.14 cm standard length). Our experimental setup used transmitted illumination with IR lights to visualize the fish with high contrast under variable levels of reflected visible light. The fish were enclosed in an arena ($\varnothing \sim 67$ cm), with a shallow water depth (13 cm). Experiments were either performed over a long duration (30 min) at a time-lapse recording rate (0.5 frames s^{-1}, 2.5 ms exposure) or for a brief duration ($6 - 10$ s) with high-speed video (500 frames s^{-1}, 2 ms exposure) on a total of 105 fish. The long-duration recordings included the entire arena (at 1536×1536 pixels) and thereby offered comprehensive measurements of position, including interactions with the enclosure wall. The high-speed recordings were intended to examine the details of intermittent swimming during schooling through the center of the tank (~ 46 cm wide at 2048×2048 pixels) and our analysis therefore included the tracking of individuals over time (figure S1*a*-*b*).

We tested the roles of the visual and lateral line systems on schooling through experimental manipulation. We varied the white light generated by two lamps, each with a single LED bulb (6 W), controlled with a variable dimmer. This allowed for video recordings of swimming under eight levels of illuminance (0, 0.44, 0.62, 0.66, 0.70, 1.25, 1.80, and 8.15 lx). The lateral-line system was manipulated through exposure to a solution of neomycin sulfate (Fisher BioReagents, Fair Lawn, NJ, USA, see Electronic Supplemental Materials for protocol). This treatment was verified in a group of animals that were not used for schooling experiments with a fluorescent vital stain for hair cells (DASPEI, 2-(4-(dumethylamino)styryl)-N-ethylpyridinium iodide, figure S1*c*). Fish in the control group were handled to the same extent as the treated fish and no anesthesia was required for the treatment. The effects of the lateral line manipulation were considered for experiments conducted at two light levels (1.80 lx and 8.15 lx) that were found to be sufficient for schooling.

The kinematics of swimming were acquired and analyzed with custom software. This software was developed in Matlab (R2018b, MathWorks, Natick, MA, USA, see Electronic Supplemental Materials for details). The automated acquisition of kinematics worked by finding the center of area for each fish, as well as the anterior margin of the rostrum, which allowed for measurements of the heading (θ, figure S1b). For short-duration experiments, we focused on the determinants of the direction and magnitude of turning during bursts by measuring how they varied with the numbers of neighbors to the left and right sides of a focal fish. We similarly measured how the change in speed during a burst varied with the numbers of fish ahead and behind the focal fish. For the long-duration recordings, we calculated the mean speed ($\overline{V}$), nearest-neighbor distance ($\overline{D}$), which we found as the mean across time of the mean among individuals. Measurements of the polarization provided a non-dimensional metric of the common alignment of the fish in a school, calculated as follows [50, 18]:

$$\rho(t) = \frac{1}{n}\sqrt{\left(\sum_{i=1}^{n}\sin\theta_i(t)\right)^2 + \left(\sum_{i=1}^{n}\cos\theta_i(t)\right)^2}, \tag{3.1}$$

where i is an index for a particular fish and n is the total number of fish in a school ($n = 5$). The mean polarization ($\overline{\rho}$) was calculated as the mean value of a school over time.

3.4 Results

Tetras schooled with intermittent bursts in speed that were frequently accompanied by changes in heading (figure 3.1a–c). During these bursts, individuals changed their position within a school and thereby generated large temporal variation of the nearest-neighbor distance and polarization (figure 3.1d–e). We found that the fish tended to swim faster when they were behind their neighbors (figure S2, table S2) and that the lateral position of neighbors had a significant effect on the kinematics of turning. In particular, the proba-

bility of turning either left or right depended on the number of neighbors on either side of a focal fish (figure 3.2*a*). When a fish was balanced by two fish on either side, they would turn toward the right with a probability indistinguishable from 50% ($p_{\mathrm{R}} = 0.52, 95\%$ CI: $0.43 - 0.60, n = 15$ over 141 experiments). When there were no fish on the right, fish tended to turn toward that side of the body only about one-third of the time ($p_{\mathrm{R}} = 0.30, 95\%$ CI: $0.23 - 0.37$) and when all four fish were on the right, turns were pointed in that direction around two-thirds of the time ($p_{\mathrm{R}} = 0.64, 95\%$ CI: $0.56 - 0.72$). These results suggest that turning decisions either considered the numbers of neighbors on opposite sides of the body or resulted from the focal fish moving away from the side of the body with no visible neighbors.

The distribution of neighbors around a focal fish affected the magnitude of changes in heading during a turn. A generalized linear mixed-effects model found that the number of fish on the side of the body in the direction of a turn showed a highly significant effect on the change in heading during a turn (figure 3.2*b*), with an estimated regression coefficient of 1.94° ($n = 15$, 141 experiments, table S1). This suggests, for example, if there were 4 fish on the left side of a focal fish, then the average left turn would be 7.76° ($4 \times 1.94°$) more than if there were no fish on the left side.

Performing experiments under different levels of illuminance allowed us to address the effects of vision on schooling. Long-duration experiments (figure S3) showed that kinematics varied with the availability of ambient light (figure 3.3*a*–*d*). In darkness and under low illuminance, fish moved with low polarization and a large mean nearest-neighbor distance that spanned many body lengths ($> 15\,\mathrm{cm}$). Under brighter light (> 1.5 lx), the mean distance (± 1 SD) between nearest neighbors dropped considerably (e.g., $\overline{D} = 6.55\,\mathrm{cm} \pm 2.37\,\mathrm{cm}$ at 1.8 lx, $N = 5$) and fish moved with a more polarized orientation (e.g., $\rho = 0.54 \pm 0.02$ at 1.8 lx, $N = 5$). The results of our high-speed kinematics showed that fish under brighter light turned to a slightly greater degree during bursts than under dim light (table S1). However, illuminance did not affect turning probability, by comparison of 95% confidence intervals

(figure 3.2*a*), or the relationship between changes in speed and the position of neighbors (figure S2, table S2).

Manipulating the lateral line system altered schooling kinematics. A 2-way ANOVA found that the manipulation significantly affected both the minimum distance ($p < 0.001$) and polarization for our long-duration recordings ($p = 0.02$, figure 3.3*e–g*). Fish schooled at a distance from their nearest neighbor that was 79% greater when they did not have the assistance of the lateral line ($\overline{D} = 10.9 \pm 4.8\,\text{cm}, n = 8$), compared to the control ($\overline{D} = 6.1 \pm 1.5\,\text{cm}, n = 18$), when we combined measurements from the two levels of illuminance. Polarization of the control groups was 15% greater on average ($\overline{\rho} = 0.52 \pm 0.07, n = 18$) than the treated fish ($\overline{\rho} = 0.45 \pm 0.04, n = 8$). Therefore, schools comprised of fish with an ability to sense flow swam more closely together and with greater similarity in heading than groups with a compromised lateral line. However, our lateral line manipulation showed no significant effects on the relationships between speed and the duration of burst and coast phases (figure S4, table S3) or on the relationships in kinematics between focal and neighboring fish (figure S5, table S4).

3.5 Discussion

Our experiments addressed the role of vision in schooling. The inability of the tetras to school in the dark (figure 3.3*a–d*) and their capacity to school with a compromised lateral line (figure 3.3*e–g*), suggest that vision is both necessary and sufficient for schooling. These results contrast the pollock's ability to school in the dark [68], but the necessity of vision is not unusual. A variety of other species are similarly incapable of schooling in darkness, including a freshwater cyprinid (*Danionella translucida*) [74], and a number of pelagic marine species (*Scomber scombrus*, *Pseudocaranx dentex*, *Thunnus orientalis*, and *Scomber scombrus L.*) [46, 85, 3]. Schooling therefore is principally facilitated by the visual system in many

fish species. The ability to school in the dark may thus be the exception, and not the norm, among fishes.

We tested the function of visual cues by measuring schooling kinematics over a range of light intensities. The nearest-neighbor distance, speed, and polarization were at similar values of illuminance above a threshold (¿ 1.5 lx). Under dimmer light, the inability to school was manifested by a greater nearest-neighbor distance and low polarization (figure 3.3*c–d*). Our results do not distinguish between whether visually-mediated polarization occurs as a consequence of attraction [51] or results from fish actively matching the heading of their neighbors [14, 94], as either mechanism could be enhanced by a stronger visual stimulus. Similar results have been observed in some marine species [61, 46, 85], which illustrates a general role for the visual system in attracting fish together when provided with sufficient illumination and water clarity.

Schooling was altered by our manipulation of the lateral line system. The lateral line is generally thought to offer information about other fishes through flow cues that emerge in relatively close spatial interactions [58]. We found that the tetras moved at a distance that was 79% greater from their nearest neighbor with a compromised lateral line than the control group (figure 3.3*f*), similar to what was previously reported [30]. This result is consistent with the idea that flow serves as an attractive sensory cue when in close proximity. In contrast, ablating the trunk lateral line in pollock [65] and the golden shiner [9] reduced the spacing between neighbors, which suggests that flow serves as a cue for repulsion. However, the ability of pollock to school in the dark [68] also indicates that flow may serve an attractive function in the same species that uses flow for repulsion. Both the lateral line and visual systems may therefore facilitate attraction at relatively large distances and repulsion in close proximity.

Differences in sensing between species may be affected by the degree by which they move intermittently [38, 70]. We found that bursts of swimming frequently caused tetras to advance

in their position in the school, which they would forfeit during the coasting phase, as the other fish accelerated (figure 3.1*a*). These persistent changes in relative position contrast the kinematics of some steady-swimming species that maintain their station in a school [51] and likely presents a fish with highly dynamic stimuli. The visual field of an intermittent swimmer is exposed to changing visual angles for its neighbors and flow stimuli should reflect the unsteady motion of conspecifics. Our results suggest that decisions about turning (figure 3.2*b*) and changes in speed (figure S2) during swimming bursts depend on the spatial distribution of neighbors, which is consistent with previous observations of the rummy-nose tetra [30, 55, 10, 48] and other intermittent swimmers [38, 43, 4, 70]. This spatial accounting apparently depends on visual cues and is likely beyond the receptive field of the lateral line [58]. Steady swimming that depends on group members in close proximity may more easily use flow as a means of information for schooling.

3.6 Summary

The present study evaluated the roles of vision and flow sensing in the schooling behavior of a species that swims intermittently. By manipulating the intensity of light, we found that vision serves to attract and align the members of a school (figure 3.3*c*-*d*). We found that vision is sufficient to school when we compromised the lateral line system, but that flow sensing draws fish together and increases polarization (figure 3.3*f*-*g*). Therefore, flow sensing in the rummy-nose tetra enhances schooling that is facilitated by the visual system.

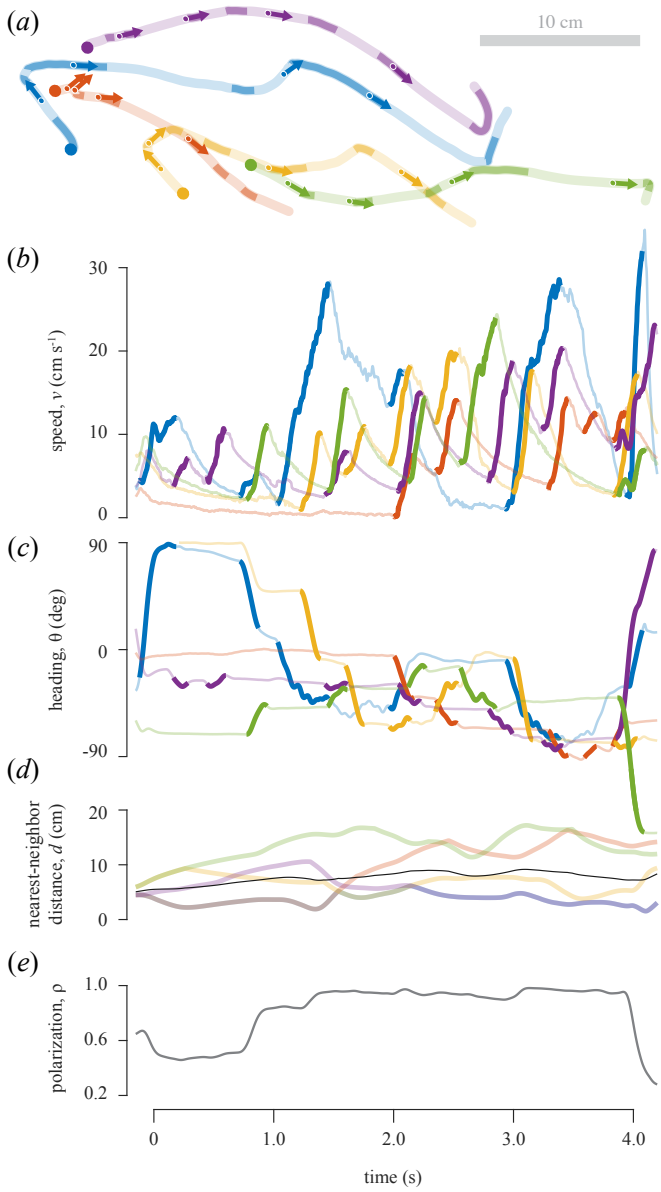

Figure 3.1: High-speed kinematics of a school of fish swimming intermittently. (a) The trajectory of each fish is displayed with a unique color, with periods of acceleration indicated by dark curves and decelerations shown in light colors, starting at each filled circle. The arrows indicate the heading of a fish at regular (1 s) intervals, starting at 0.5 s. (b–e) Time series of measurements for the trajectories shown in a. (b) Periods of bursts (dark curves) and coasts (light curves) were found with an automated approach from these measurements of speed. (c) Variation in heading reflects the intermittent changes in direction that were correlated with the bursting phase. (d) The nearest-neighbor distance is indicated with curves that show the shared values between neighbors and the mean among all members (black curve). (e) Polarization was calculated from the heading values in c (Eqn. 3.1) and indicates the common alignment of fish in the group.

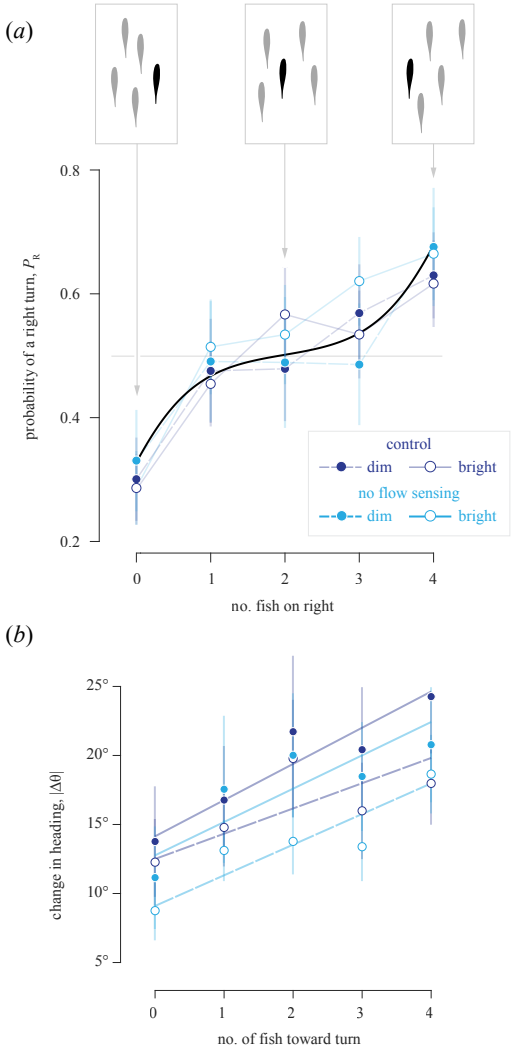

Figure 3.2: Changes in heading relative to the position of neighboring fish. Measurements are shown for four neomycin-treated (i.e., 'no flow sensing', red, $n = 8$) and control (blue, $n = 8$) groups under dim (1.80 lx, filled circles) and bright (8.15 lx, open circles) light for $92 - 236$ turns, depending on the group. (a) Probability of turning toward the right, as a function of the number of fish to the left:right of the focal fish ($\pm$95% confidence intervals, assuming binomial distribution). (b) The change in heading during turns is shown with respect to the number of neighboring fish in the direction of the turn (mean $\pm$95% confidence intervals, assuming normal distribution) with trend lines for our generalized linear mixed-effects model for experiments under bright (dashed line, $r^2 = 0.76$) and dim (solid line, $r^2 = 0.82$) light (see table S1 for statistics).

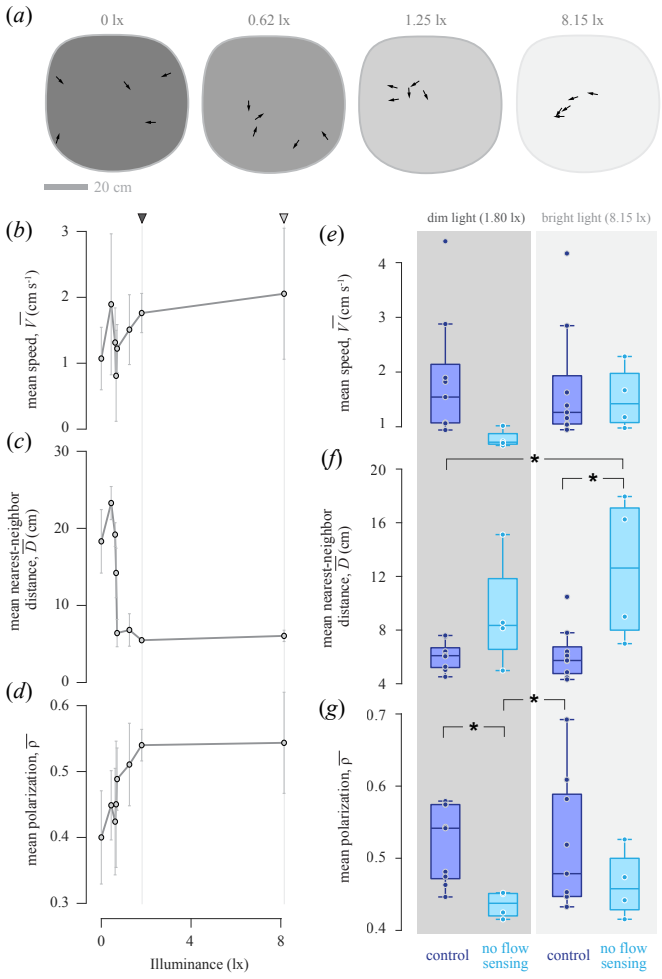

Figure 3.3: The effects of light and flow sensing on schooling kinematics for long-duration recordings. (a) Arrows denote the position and orientation of fish from video stills of experiments performed at different levels of illuminance. (b–d) Measurements of schooling kinematics among multiple schools under varying light intensity. Triangles above the panels and vertical lines designate the light intensities at which we performed additional experiments at dim (dark gray) and bright (light gray) light. Circles indicate the mean value (± 1 SD) for the (b) mean speed, (c) mean nearest-neighbor distance, and (d) polarization among the schools ($3 < n < 5$). (e-g) The effects of lateral line manipulation on schooling kinematics at two light intensities. The (e) mean speed, (f) nearest-neighbor distance, and (g) polarization among experiments performed under dim (dark gray area, 1.80 lx) and bright (light gray area, 8.15 lx) light. Fish were either treated such that their lateral line system was compromised (red), or served as a control (blue). The box plots indicate the values for individual groups (circles, $4 < n < 8$), the median value (center line), with the box designating the first and and third quartiles and the range indicated by the error flags. Values for the mean speed (b,e) and mean nearest-neighbor distance (c,f) were calculated as the mean over time of the mean value among individuals for a school. Significant differences between groups ($p < 0.05$) indicated by the asterisks, as found by 2-way ANOVA with post-hoc tests.

Bibliography

[1] L. Abbas and T. T. Whitfield. The zebrafish inner ear. *Fish Physiology*, 29:123–171, 2010.

[2] J. M. Ache, J. Polsky, S. Alghailani, D. D. Bock, C. R. von Reyn, and G. M. Card. Neural basis for looming size and velocity encoding in the drosophila giant fiber escape pathway. *Current Biology*, 29(6):1073–1081, 2019.

[3] M. Ali. The ocular structure, retinomotor and photo-behavioral responses of juvenile pacific salmon. *Can. J. Zool.*, 37(1959):965–996, 2001.

[4] S. Arganda, A. Pérez-Escudero, and G. G. De Polavieja. A common rule for decision making in animal collectives across species. *Proc. Nat. Acad. Sci.*, 109:20508–20513, 2012.

[5] I. Ashraf, H. Bradshaw, T. T. Ha, J. Halloy, R. Godoy-Diana, and B. Thiria. Simple phalanx pattern leads to energy saving in cohesive fish schooling. *Proc. Nat. Acad. Sci.*, 114:9599–9604, 2017.

[6] K. Bhattacharyya, D. L. McLean, and M. A. MacIver. Visual threat assessment and reticulospinal encoding of calibrated responses in larval zebrafish. *Current Biology*, 27:2751–2762, 2017.

[7] C. Breder. Equations descriptive of fish schools and other animal aggregations. *Ecology*, 35:361–370, 1954.

[8] H. A. Burgess and M. Granato. Modulation of locomotor activity in larval zebrafish during light adaptation. *Journal of Experimental Biology*, 210:2526–2539, 2007.

[9] J. W. Burgess and E. Shaw. Effects of Acoustico-Lateralis Denervation in a Facultative Schooling Fish : A Nearest-Neighbor Matrix Analysis. *Behav. Neural Biol.*, 497:488–497, 1981.

[10] D. S. Calovi, A. Litchinko, V. Lecheval, U. Lopez, A. Pérez Escudero, H. Chaté, C. Sire, and G. Theraulaz. Disentangling and modeling interactions in fish with burst-and-coast swimming reveal distinct alignment and attraction behaviors. *PLoS Comp. Biol.*, 14:1–28, 2018.

[11] A. Carrillo, D. V. Le, M. Byron, H. Jiang, and M. J. McHenry. Canal neuromasts enhance foraging in zebrafish (danio rerio). *Bioinspiration and Biomimetics*, 14:035003, 2019.

[12] A. Carrillo and M. McHenry. Zebrafish learn to forage in the dark. *Journal of Experimental Biology*, 219:582–589, 2016.

[13] J. Clery, O. Guipponi, S. Odouard, S. Pinede, C. Wardak, and S. Ben Hamed. The prediction of impact of a looming stimulus onto the body is subserved by multisensory integration mechanisms. *Journal of Neuroscience*, 37(44):10656–10670, 2017.

[14] B. Collignon, A. Séguret, and J. Halloy. A stochastic vision-based model inspired by zebrafish collective behaviour in heterogeneous environments. *Roy. Soc. Open Sci.*, 3(1), 2016.

[15] S. A. Combes, D. E. Rundle, I. J. M, and C. J. D. Linking biomechanics and ecology through predator prey interactions: flight performance of dragonflies and their prey. *The Journal of Experimental Biology*, 215(6):903–913, 2012.

[16] W. E. J. Cooper and D. T. Blumstein. *Escaping From Predators: An Integrative View of Escape Decisions*. Cambridge University Press, 2015.

[17] S. O. Coronel, N. Martorell, M. Beron de Astrada, and V. Medan. Stimulus contrast information modulates sensorimotor decision making in goldfish. *Frontiers in Neural Circuits*, 14:23, 2020.

[18] I. D. Couzin, J. Krause, R. James, G. D. Ruxton, and N. R. Franks. Collective memory and spatial sorting in animal groups. *J. Theor. Biol.*, 218:1–11, 2002.

[19] R. L. Day, T. MacDonald, C. Brown, K. N. Laland, and S. M. Reader. Interactions between shoal size and conformity in guppy social foraging. *Anim. Behav.*, 62:917–925, 2001.

[20] S. W. Day, T. E. Higham, A. Y. Cheer, and P. C. Wainwright. Spatial and temporal patterns of water flow generated by suction-feeding bluegill sunfish resolved by Particle Image Velocimetry. *Journal of Experimental Biology*, 208:2661–2671, 2005.

[21] N. Y. Dektyareva, R. S. Shtanchayev, G. Z. Mikhailova, and D. A. Moshkov. Stabilization of motor asymmetry in the goldfish under the influence of optokinetic stimulation. *Neurophysiology*, 40(3):178–186, 2008.

[22] S. Dijkgraaf. The functioning and significance of the lateral-line organs. *Biological Reviews*, 38(1):51–105, 1963.

[23] L. M. Dill. Visual mechanism determining flight distance in zebra danios (brachydanio rerio pisces). *Nature*, 236:30–32, 1971.

[24] L. M. Dill. The escape response of the zebra danio (brachydanio rerio) i. the stimulus for escape. *Animal Behavior*, 22:711–722, 1974.

[25] P. Domenici, J. M. Blagburn, and J. P. Bacon. Animal escapology i: theoretical issues and emerging trends in escape trajectories. *Journal of Experimental Biology*, 214(15):2463–2473, 2011.

[26] P. Domenici, J. M. Blagburn, and J. P. Bacon. Animal escapology ii: escape trajectory case studies. *Journal of Experimental Biology*, 214(15):2474–2494, 2011.

[27] T. W. Dunn, C. Gebhardt, E. A. Naumann, C. Riegler, M. B. Ahrens, F. Engert, and F. Del Bene. Neural circuits underlying visually evoked escapes in larval zebrafish. *Neuron*, 89:613–628, 2016.

[28] S. S. Easter and G. N. Nicola. The development of vision in the zebrafish (*Danio rerio*). *Developmental Biology*, 180(0335):646–663, 1996.

[29] R. C. Eaton and A. N. Popper. The octavolateralis system and mauthner cell: interactions and questions. *Brain Behavioral and Evolution*, 46:124–130, 1995.

[30] K. Faucher, E. Parmentier, C. Becco, N. Vandewalle, and P. Vandewalle. Fish lateral system is required for accurate control of shoaling behaviour. *Anim. Behav.*, 79:679–687, 2010.

[31] J. R. Fetcho. Spinal network of the mauthner cell. *Brain Behavior Evolution*, 37:298–316, 1991.

[32] M. B. Foreman and R. C. Eaton. The direction change concept for reticulospinal control of goldfish escape. *The Journal of Neuroscience*, 13(10):4101–4113, 1993.

[33] S.-J. Fu. Flow and stress acclimation both enhance predator avoidacne in common cyprinid fish. *Aquatic Biology*, 24(1):1–8, 2015.

[34] F. Gabbiani, H. G. Krapp, and G. Laurent. Computation of object approach by a wide-field, motion-sensitive neuron. *Journal of Neuroscience*, 19:1122–1141, 1999.

[35] J. Gautrais, F. Ginelli, R. Fournier, S. Blanco, M. Soria, H. Chaté, and G. Theraulaz. Deciphering interactions in moving animal groups. *PLoS Comp. Biol.*, 8, 2012.

[36] J.-G. J. Godin, L. J. Classon, and M. V. Abrahams. Group vigilance and shoal size in a small characin fish. *Behavior*, 104:29–40, 1988.

[37] S. Grillner and A. E. Manira. Current principles of motor control with special reference to vertebrate locomotion. *Physiological Reviews*, 100:271–320, 2020.

[38] R. Harpaz, G. Tkačik, and E. Schneidman. Discrete modes of social information processing predict individual behavior of fish in a group. *Proc. Nat Acad. Sci.*, 114(38):10149–10154, 2017.

[39] J. A. Harris, A. G. Cheng, L. L. Cunningham, and M. G. Neomycin-induced hair cell death and rapid regeneration in the laterl line of zebrafish *Danio rerio*. *J. Assoc. Res. Otolaryn.*, 4:219–234, 2003.

[40] T. E. Higham. Feeding, fins and braking maneuvers: locomotion during prey capture in centrarchid fishes. *Journal of Experimental Biology*, 210:107–117, 2007.

[41] T. E. Higham, B. Malas, B. C. Jayne, and G. V. Lauder. Constraints on starting and stopping: behavior compensates for reduced pectoral fin area during braking of the bluegill sunfish Lepomis macrochirus. *Journal of Experimental Biology*, 208(24):4735–4746, 2005.

[42] T. E. Higham, W. J. Stewart, and P. C. Wainwright. Turbulence, temperature, and turbidity: the ecomechanics of predator-prey interactions in fishes. *Integrative and Comparative Biology*, 55(1):6–20, 2015.

[43] R. C. Hinz and G. G. de Polavieja. Ontogeny of collective behavior reveals a simple attraction rule. *Proc. Nat. Acad. Sci.*, 114:2295–2300, 2017.

[44] Y. Hochberg and A. C. Tamhane. *Multiple Comparison Procedures*. John Wiley & Sons, Ltd, Hoboken, NJ, 1987.

[45] R. Holzman, S. W. Day, and P. C. Wainwright. Timing is everything: coordination of strike kinematics affects the force exerted by suction feeding fish on attached prey. *Journal of Experimental Biology*, 210:3328–3336, 2007.

[46] J. R. Hunter. Effects of light on schooling and feeding of jack mackerel, *Trachurus symmetricus*. *J. Fish. Res. Board Canada*, 25:393–407, 1968.

[47] R. Isaacs. *Differential Games. A Mathematical Theory with Applications to Warfare and Pursuit, Control and Optimization*. John Wiley & Sons, Inc., New York, 1965.

[48] L. Jiang, L. Giuggioli, A. Perna, R. Escobedo, V. Lecheval, C. Sire, Z. Han, and G. Theraulaz. Identifying influential neighbors in animal flocking. *PLoS Comp. Biol.*, 13(11):1–32, 2017.

[49] K. R. John. Illumination, vision, and schooling of astyanax mexicanus (fillipi). *J. Fish. Res. Board Can.*, 21:1453–1473, 1964.

[50] J. W. Jolles, N. J. Boogert, V. H. Sridhar, I. D. Couzin, and A. Manica. Consistent individual differences drive collective behavior and group functioning of schooling fish. *Curr. Biol.*, 27(18):2862–2868.e7, 2017.

[51] Y. Katz, K. Tunstrom, C. C. Ioannou, C. Huepe, and I. D. Couzin. Inferring the structure and dynamics of interactions in schooling fish. *Proc. Nat. Acad. Sci.*, 108:18720–18725, 2011.

[52] T. Kohashi, N. Nakata, and Y. Oda. Effective sensory modality activating an escape triggering neuron switches during early development in zebrafish. *Journal of Neuroscience*, 32(17):5810–5820, 2012.

[53] A. M. B. Lacoste, D. Schoppik, F. Engert, and A. F. Schier. A convergent and essential interneuron pathway for mauthner-cell-mediated escapes. *Current Biology*, 25:1526–1534, 2015.

[54] S. M. Leber and P. G. Model. Effect of preccious and delayed afferent arrival on synapse localization on the amphibian mauthner cell. *Journal of Comparative neurology*, 313(1):31–44, 1991.

[55] V. Lecheval, L. Jiang, P. Tichit, C. Sire, C. K. Hemelrijk, and G. Theraulaz. Social conformity and propagation of information in collective u-turns of fish schools. *Proc. Roy Soc. B*, 285(1877), 2018.

[56] M. Lin and H. A. Nash. Influence of general anesthetics on a specific neural pathway in *Drosophila melanogaster*. *Proceedings of the National Academy of Sciences of the United States of America*, 93(19):10446–10451, 1996.

[57] M. J. McHenry, K. E. Feitl, J. A. Strother, and W. J. V. Trump. Larval zebrafish rapidly sense the water flow of a predator's strike. *Biology Letters*, 5:477–479, 2009.

[58] M. J. McHenry and J. C. Liao. The Hydrodynamics of Flow Stimuli. In S. Coombs, H. Bleckmann, R. R. Fay, and A. N. Popper, editors, *The Lateral Line*, volume 48, page 26. Springer, New York.

[59] P. J. Mekdara, M. A. B. Schwalbe, L. L. Coughlin, and E. D. Tytell. The effects of lateral line ablation and regeneration in schooling giant danios. *J. Exp. Biol.*, 221:jeb.175166, 2018.

[60] G. A. Milliken and D. E. Johnson. *Analysis of Messy Data. Volume I: Designed Experiments.* Chapman & Hall/CRC Press, Boca Raton, FL, 1992.

[61] T. Miyazaki, S. Shiozawa, T. Kogane, R. Masuda, K. Maruyama, and K. Tsukamoto. Developmental changes of the light intensity threshold for school formation in the striped jack Pseudocaranx dentex. *Mar. Ecol. Prog. Ser.*, 192:267–275, 2000.

[62] D. A. Moshkov, L. L. Pavlik, N. R. Tiras, D. A. Dzeban, and I. B. Mikheeva. Ultrastructural changes in the mixed synapses of mauthner neurons related to long-term potentiation and natural modification of the motor function. *Neurophysiology*, 35(5):361–370, 2003.

[63] A. Nair, K. Changsin, W. J. Stewart, and M. J. McHenry. Fish prey change strategy with the direction of a threat. *Proceedings of the Royal Society B*, 284(1857):20170393, 2017.

[64] D. Oliva and D. Tomsic. Visuo-motor transformations involved in the escape response to looming stimuli in the crab neohelice (=chasmagnathus) granulata. *Journal of Experimental Biology*, 215(19):3488–3500, 2012.

[65] B. L. Partridge and T. J. Pitcher. The sensory basis of fish schools: relative roles of lateral line and vision. *J .Comp. Phys. A*, 135:315–325, 1980.

[66] D. Pita, B. A. Moore, L. P. Tyrrell, and E. Fernández-Juricic. Vision in two cyprinid fish: implications for collective behavior. *PeerJ*, 3(e1113):doi:10.7717/peerj.1113, 2015.

[67] T. J. Pitcher. Heuristic definitions of fish shoaling behaviour. *Anim. Behav.*, 31:611–613, 1983.

[68] T. J. Pitcher, B. L. Partridge, and C. Wardle. A blind fish can school. *Science*, 194:963–965, 1976.

[69] T. Preuss, P. E. Osei-Bonsu, S. A. Weiss, C. Wang, and D. Faber. Neural representation of object approach in a decision-making motor circuit. *Journal of Neuroscience*, 26(13):3454–3464, 2006.

[70] J. G. Puckett, A. R. Pokhrel, and J. A. Giannini. Collective gradient sensing in fish schools. *Sci. Reports*, 8:1–11, 2018.

[71] O. Randlett, M. Haesemeyer, G. Forkin, H. Shoenhard, A. F. Shier, F. Engert, and M. Granato. Distributed plasticity drives visual habituation learning in larval zebrafish. *Current Biology*, 29(8):1337–1345, 2019.

[72] R. D. Santer, Y. Yamawaki, F. C. Rind, and P. J. Simmons. Preparing for escape: an examination of the role of the dcmd neuron in locust escape jumps. *Journal of Comparative Physiology*, 194:69–77, 2008.

[73] W. Schiff, J. A. Caviness, and J. J. Gibson. Persistent fear responses in rhesus monkeys to the optical stimulus of looming. *Science*, 136:982–983, 1962.

[74] L. Schulze, J. Henninger, M. Kadobianskyi, T. Chaigne, A. I. Faustino, N. Hakiy, S. Albadri, M. Schuelke, L. Maler, F. Del Bene, and B. Judkewitz. Transparent Danionella translucida as a genetically tractable vertebrate brain model. *Nature Methods*, 15:977–983, 2018.

[75] P. Silver. Photopic spectral sensitivity of the neon tetra *Paracheirodon innesi* (Myers) found by the use of a dorsal light reaction. *Vision Res.*, 14:329–334, 1973.

[76] A. Soto, W. J. Stewart, and M. J. McHenry. When optimal strategy matters to prey fish. *Integrative and Comparative Biology*, 55(1):1–11, 2015.

[77] W. J. Stewart, G. S. Cardenas, and M. J. McHenry. Zebrafish larvae evade predators by sensing water flow. *The Journal of Experimental Biology*, 216(3):388–398, 2013.

[78] W. J. Stewart and M. J. McHenry. Sensing the strike of a predator fish depends on the specific gravity of a prey fish. *Journal of Experimental Biology*, 213:3769–3777, 2010.

[79] W. J. Stewart, A. Nair, J. Houshuo, and M. J. McHenry. Prey fish escape by sensing the bow wave of a predator. *Journal of Experimental Biology*, 217:4328–4336, 2014.

[80] W. J. Stewart, A. Nair, H. Jiang, and M. J. McHenry. Prey fish escape by sensing the bow wave of a predator. *Journal of Experimental Biology*, 217(24):4328–4336, 2014.

[81] H. Straka and R. Baker. *HEARING AND LATERAL LINE — Vestibular System Anatomy and Physiology.* Academic Press, San Diego, 2011.

[82] L. F. Tammero and M. H. Dickinson. Collision-avoidance and landing responses are mediated by separate pathways in the fruit fly, *Drosophila melanogaster*. *Journal of Experimental Biology*, 205:2785–2798, 2002.

[83] I. Temizer, J. C. Donovan, H. Baier, and J. L. Semmelhack. A visual pathway for looming evoked escape in larval zebrafish. *Current Biology*, 25:1823–1834, 2015.

[84] M. Timmermann, I. Schlupp, and M. Plath. Shoaling behaviour in a surface-dwelling and a cave-dwelling population of a barb *Garra barreimiae* (Cyprinidae, Teleostei). *Acta Ethologica*, 7(2):59–64, 2004.

[85] S. Torisawa, T. Takagi, H. Fukuda, Y. Ishibashi, Y. Sawada, T. Okada, S. Miyashita, K. Suzuki, and T. Yamane. Schooling behaviour and retinomotor response of juvenile Pacific bluefin tuna Thunnus orientalis under different light intensities. *J. Fish Biol.*, 71:411–420, 2007.

[86] W. J. Van Trump, S. Coombs, K. Duncan, and M. J. McHenry. Gentamicin is ototoxic to all hair cells in the fish lateral line system. *Hear. Res.*, 261(1-2):42–50, 2010.

[87] P. C. Wainwright, L. A. Ferry-Graham, T. B. Waltzek, A. M. Carroll, C. D. Hulsey, and J. R. Grubich. Evaluating the use of ram and suction during prey capture by cichlid fishes. *Journal of Experimental Biology*, 204(17):3039–3051, 2001.

[88] Y. Wang and B. Frost. Time to collision is signaled by neurons in the nucleaus rotundus of pigeons. *Nature*, 356(6366):236–238, 1992.

[89] J. F. Webb and J. E. Shirey. Postembryonic development of the cranial lateral line canals and neuromasts in zebrafish. *Developmental Dynamics*, 228:370–385, 2003.

[90] D. Weihs. A hydrodynamical analysis of fish turning manoeuvres. *Proceedings of the Royal Society B*, 182:59–72, 1972.

[91] D. Weihs and P. W. Webb. Optimal avoidance and evasion tactics in predator-prey interactions. *Journal of Theoretical Biology*, 106:189–206, 1984.

[92] M. Westerfield. *The zebrafish book: A guide for the laboratory use of zebrafish (Brachydanio rerio)*. Eugene, OR, 1993.

[93] G. N. Wilkinson and C. E. Rogers. Symbolic description of factorial models for analysis of variance. *J. Royal Stat. Soc.*, 22:392–399, 1973.

[94] A. K. Zienkiewicz, F. Ladu, D. A. Barton, M. Porfiri, and M. D. Bernardo. Data-driven modelling of social forces and collective behaviour in zebrafish. *J. Theor. Biol.*, 443:39–51, 2018.

Appendix A

Chapter One Supplemental Material

We analyzed the responses of prey to the rate of change of the visual angle (θ') of a looming stimulus. The consensus of the contemporary literature favors the visual angle as more predictive of an escape than its rate [83, 27, 69, 6]. Nonetheless, the rate of change was previously considered the primary cue to initiate a startle response [24] and may provide a high-order influence on the timing of an escape [27, 6]. We additionally performed this analysis to demonstrate the ability of our analytical approach to consider sensory cues other than the visual angle.

In the analysis outlined in Methods, we considered the maximum possible value for a sensory cue to bound the theoretical possibilities. To find the maximum value for the threshold rate of change for the visual-angle, we solved Eqn. 2 where $t_{\text{thresh}} = -t_{\text{lat}}$ to yield the following relationship:

$$(\theta'_{\text{thresh}})_{\max} = \frac{4wu}{w^2 + 4t_{\text{lat}}^2 u^2}. \tag{A.1}$$

Finding the escape distance for a threshold value of the visual-angle rate required consideration of the timing of the escape. For this, we solved Eqn. 2 for the visual angle as a function

of time ($\theta(t)$), zero equal to the time-to-collision, and negative time values on the approach. Using this equation, we found the first-derivative of the visual angle with respect to time to calculate the time at which the threshold-stimulus angle rate was reached:

$$t_{\text{thresh}} = -\frac{\sqrt{w(4u - w\theta'_{\text{thresh}})}}{2u\sqrt{\theta'_{\text{thresh}}}}. \tag{A.2}$$

The distance between the predator and prey was calculated ($d_{\text{resp}} = -u(t_{\text{thresh}} + t_{\text{lat}})$) for the moment at which the prey initiated their escape at varying threshold values.

As performed for the visual angle (Fig. 3), we determined the threshold values for the latency and visual-angle rate of change in response to an artificial stimulus (Fig. A.1). We calculated the visual-angle rate of change discretely from measurements of the visual angle that were smoothed with a spline (the 'spaps' function in MATLAB). This entailed finding the best fit to the unity line over a range of values (15.3 deg $s^{-1} < \theta'_{\text{thresh}} < 27.5$ deg s^{-1}, $17 < N < 26$) that corresponded to the average of values for latency (830 ms $< t_{\text{lat}} <$ 850 ms) that were about one-tenth of a second longer than obtained for the visual angle.

The behavioral responses to the artificial stimulus was tested against experiments with a live predator. The results for the threshold visual-angle rate of change found variation between quartiles of -481.6 deg s^{-1} and 511.1 deg s^{-1} in response to the live predator (Fig. A.2B). This wide range of variation included all the values measured in response to the projected stimulus with a high coefficient of determination (15.3 deg $s^{-1} < \theta'_{\text{thresh}} <$ 27.5 deg s^{-1}). This indicates general agreement between the results of the two types of experiments and is consistent with previous estimates of 24.6 deg s^{-1} ($t_{\text{lat}} = 0$ ms) [24].

We modeled the kinematics of predator and prey where the prey responds to a threshold value of the rate of change in the visual angle. Simulation results suggested that zebrafish escaped at a minimum distance that shows a low likelihood of escape, regardless of the predator's speed (Fig. A.3). This suggests that the visual-angle rate of change does not offer

a robust sensory cue for successful evasion, which is unlike what is predicted for the visual angle (Fig. 5).

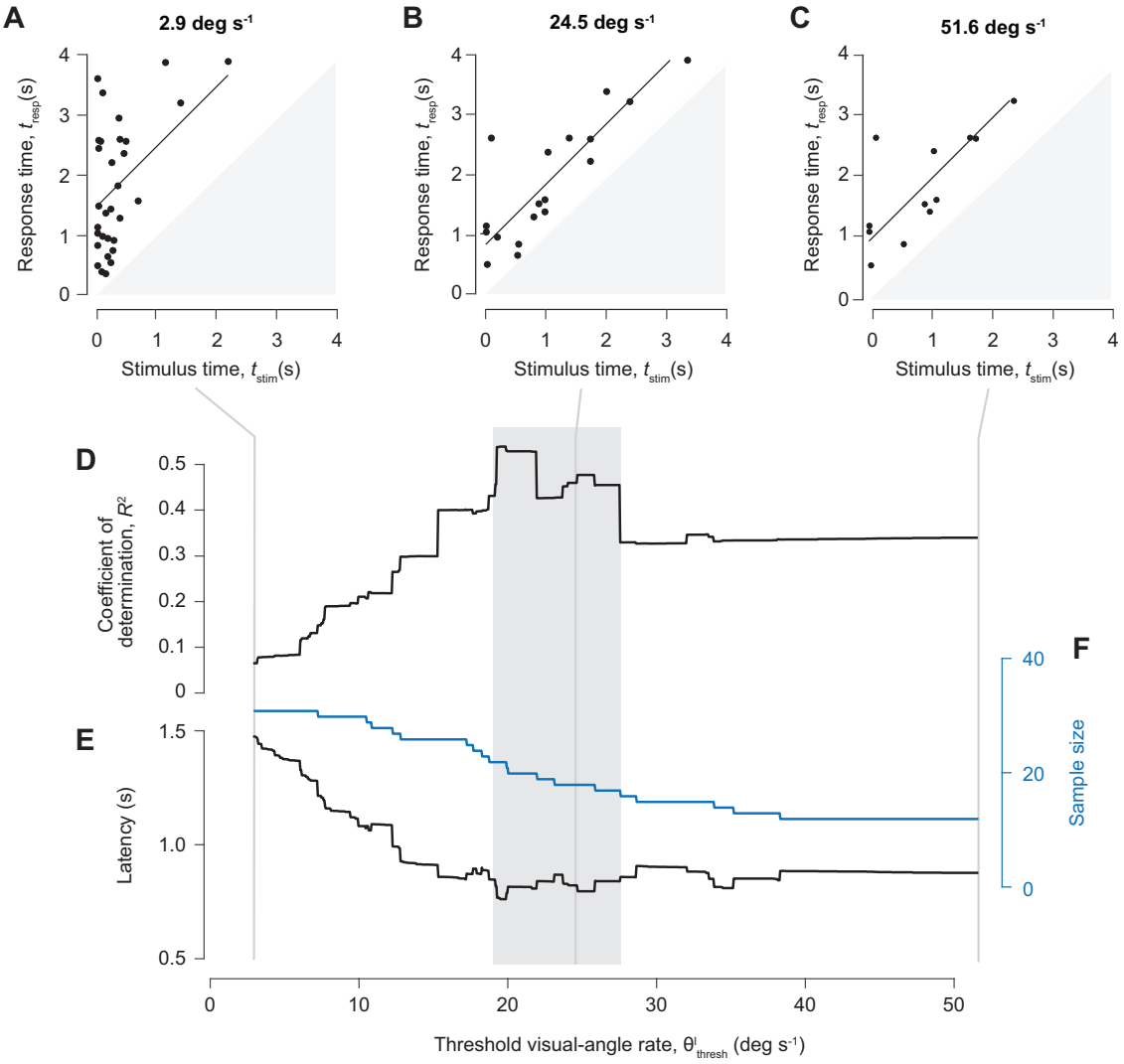

Figure A.1: Determination of the threshold visual-angle rate of change for experimental responses to the projected looming stimulus. (A–C) Relationship between the stimulus and response times, assuming three different values for the threshold visual angle rate. As described in the present manuscript (Fig. 3), this relationship should conform to a slope of unity and y-intercept equal to the latency predicted for each value of the threshold-stimulus angle rate . (D) The coefficient of determination for the unity-line fit for each value of the threshold-stimulus angle rate , (E) the corresponding latency, and (F) sample size (blue). We selected values for latency and the threshold visual-angle rate of change where the coefficient of determination was relatively high (gray bar) for comparison with responses to a live predator (Fig. A.2).

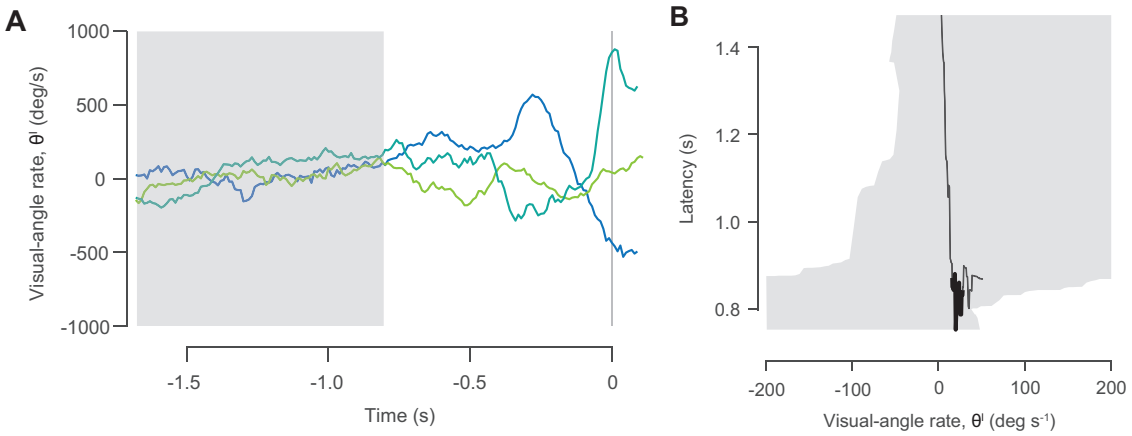

Figure A.2: Responses to a live predator. (A–B) Representative measurements of the visual angle and its rate, with time calculated relative to the response time (gray line). We considered all values for the range of latency (gray bars) suggested by measured responses to a projected stimulus (Fig. A.1). (C–D) Comparison of measurements from the projected-stimulus experiments (black curves) and live-predator experiments (gray areas) for the threshold-stimulus angle rate for the (C) visual angle and (D) its rate. The margins for the live predator are the first and third quartiles of values for the threshold-stimulus angle rate at each value for the latency. The regions of the threshold-stimulus angle rate with a high coefficient of determination (gray bars in Fig. A.1) which fall within the bounds of the live-predator experiments are highlighted (heavy black curves).

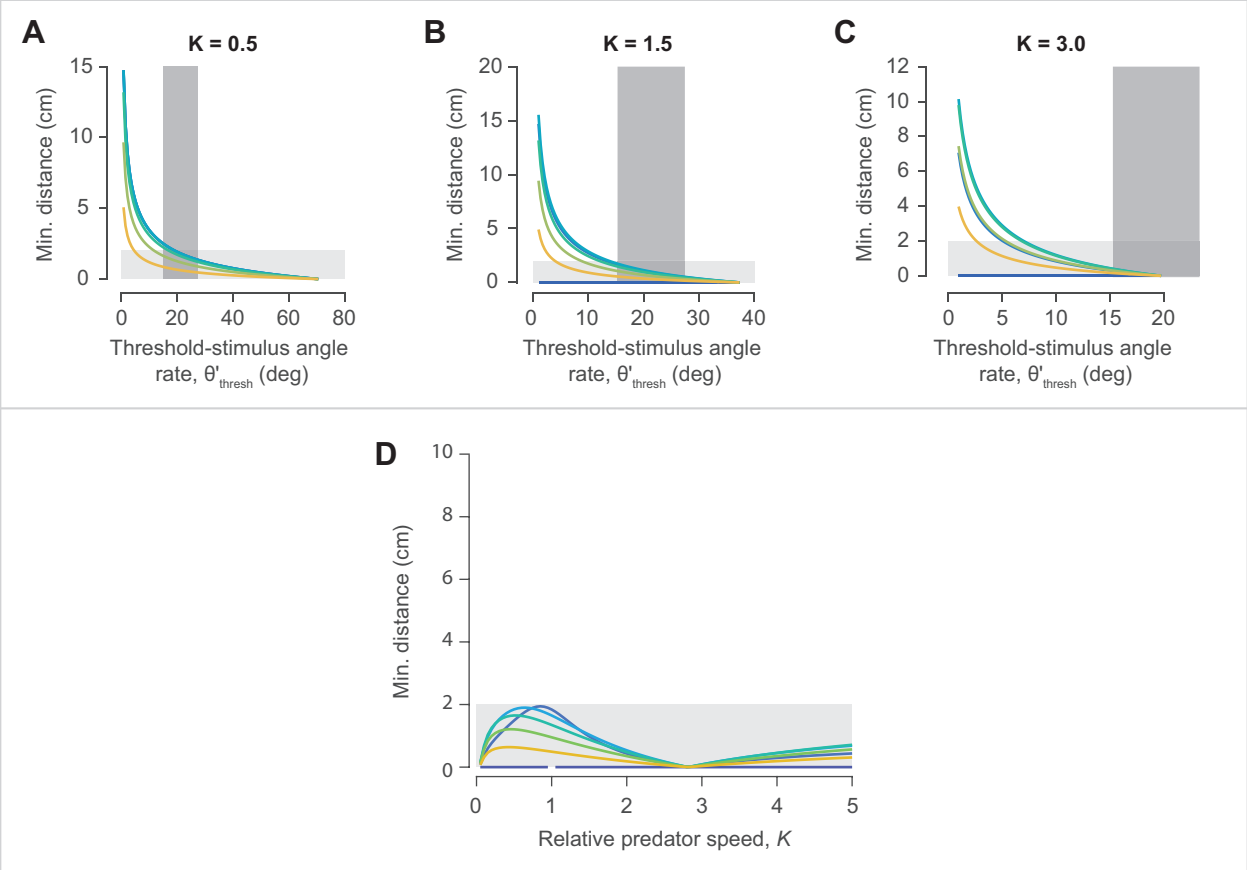

Figure A.3: The effects of the threshold-stimulus angle rate on the evasion strategy of zebrafish. (A–C) The minimum distance predicted (Eqn. 5) for varying threshold values for the rate of change of the visual angle. The vertical bars (dark gray) indicate the range of threshold values favored by our analysis of experiments (Fig. A.2) the horizontal bars (light gray) indicate distance values where the prey have a low probability of escape ($d_{\min} < 2$ cm). Calculations were performed for predators of variable relative speed ($K = 0.5$, $K = 1.5$, and $K = 3.0$). (D) The minimum distance as a function of relative predator speed at particular values of the threshold visual angle rate ($\theta_{\text{thresh}} = 21$ deg s^{-1}).

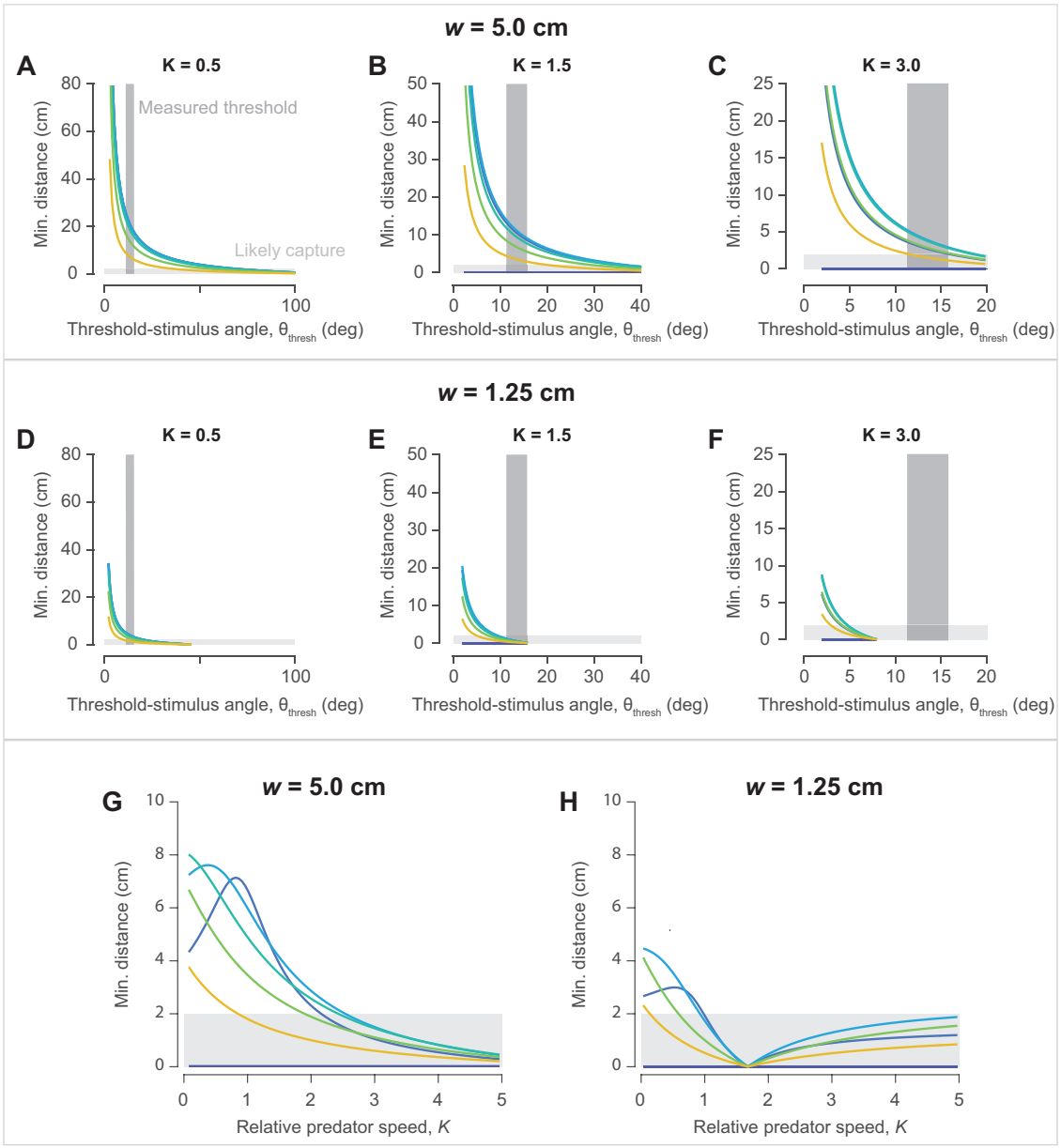

Figure A.4: The effects of the threshold-stimulus angle on the evasion strategy of zebrafish for predators of different size. (A–F) The minimum distance predicted (Eqn. 5) for varying threshold values for the rate of change of the visual angle. The vertical bars (dark gray) indicate the range of threshold values favored by our analysis of experiments (Fig. A.2) the horizontal bars (light gray) indicate distance values where the prey have a low probability of escape ($d_{\min} < 2$ cm). Calculations were performed for predators of variable relative speed ($K = 0.5$, $K = 1.5$, and $K = 3.0$). Calculations were performed for a relatively wide predator ($w = 5.00$ cm, A–C) and a relatively narrow predator ($w = 1.25$ cm, D–F). (G–H) The minimum distance as a function of relative predator speed at particular values of the threshold-stimulus angle rate ($\theta_{\text{thresh}} = 21$ deg s^{-1}) for a relatively wide predator ($w = 5.00$ cm, G) and a relatively narrow predator ($w = 1.25$ cm, H).

Appendix B

Chapter Three Supplemental Material

Methods

Animal care

We acquired adult rummy-nose tetra (*Hemmigrammus rhosostomus*) from the aquarium trade. The fish were held in a flow-through tank system (Aquatic Habitats, Apopka, FL, USA) in groups of $5-8$ fish in 3 L containers at 27° C on a 14:10 h light:dark cycle with daily feeding. Groups of 5 fish were transferred from the flow-through system into an experimental tank and allowed to acclimate (>30 min) prior to video recording. All rearing and experimental protocols were conducted with the approval of the Institutional Animal Care and Use Committee at the University of California, Irvine (IACUC Protocol #AUP-17-012).

Experimental setup and video recordings

We recorded the spontaneous swimming of fish in groups. The experimental tank included a cylindrical enclosure ($\varnothing \sim 67\,\mathrm{cm}$), a shallow water depth (13 cm), and a transparent acrylic floor (figure B.1*a*). A large mirror positioned below the tank at a 45° angle allowed a high speed camera (FastCam SA2, Photron, San Diego, CA, USA) to record the behavior of the fish from below. Videos were captured using the Photron software (FASTCAM Viewer 3, Photron, with 28 mm lens) and stored on a RAID disk-array.

An arrangement of lights provided high-contrast images of the fish while exposing them to a variable intensity of visible light. The high-contrast illumination was provided by infrared LED lamps (IR Illuminator CM-IR200, Houston, Tx, USA; 850 nm) arranged at an oblique angle to a diffuser that was positioned above the tank (figure B.1*a*). The LED lights were visible to the camera, but presumably not to the fish due to prior research [75] and our preliminary results, which indicated an inability to school under IR illumination. White light was provided by two lamps above the diffuser that were positioned close to, and directed toward, the ceiling of the room. These lamps were dimmable, each with a single LED bulb of modest maximum power (6 W) and showed no flicker when recorded with high-speed video at 1000 Hz. These bulbs provided a diffuse source of visible light that did not noticeably alter the contrast of the video images, which was dominated by the IR illumination. We measured the illuminance generated just above the experimental tank at variable dimmer settings using a light meter (L-758 Cine, Sekonic Corp., Tokyo, Japan) positioned at the tank's center, with the IR lights turned off.

In separate experiments, we recorded swimming over a long-duration or with high-speed video over a short duration. The long-duration recordings were recored at a time-lapse frame rate (0.5 frames s^{-1}, 2.5 ms exposure) that offered comprehensive kinematic measurements that viewed the entire cylindrical arena ($\sim$ 70 cm wide at 1536×1536 pixels),

including interactions with the wall. The high-speed recordings (500 frames s^{-1}, 2 ms exposure) were focused on the center of the tank ($\sim$ 46 cm wide at 2048×2048 pixels) and permitted individual tracking and a detailed view of the spatial interactions between fish during schooling (figure B.1*b*).

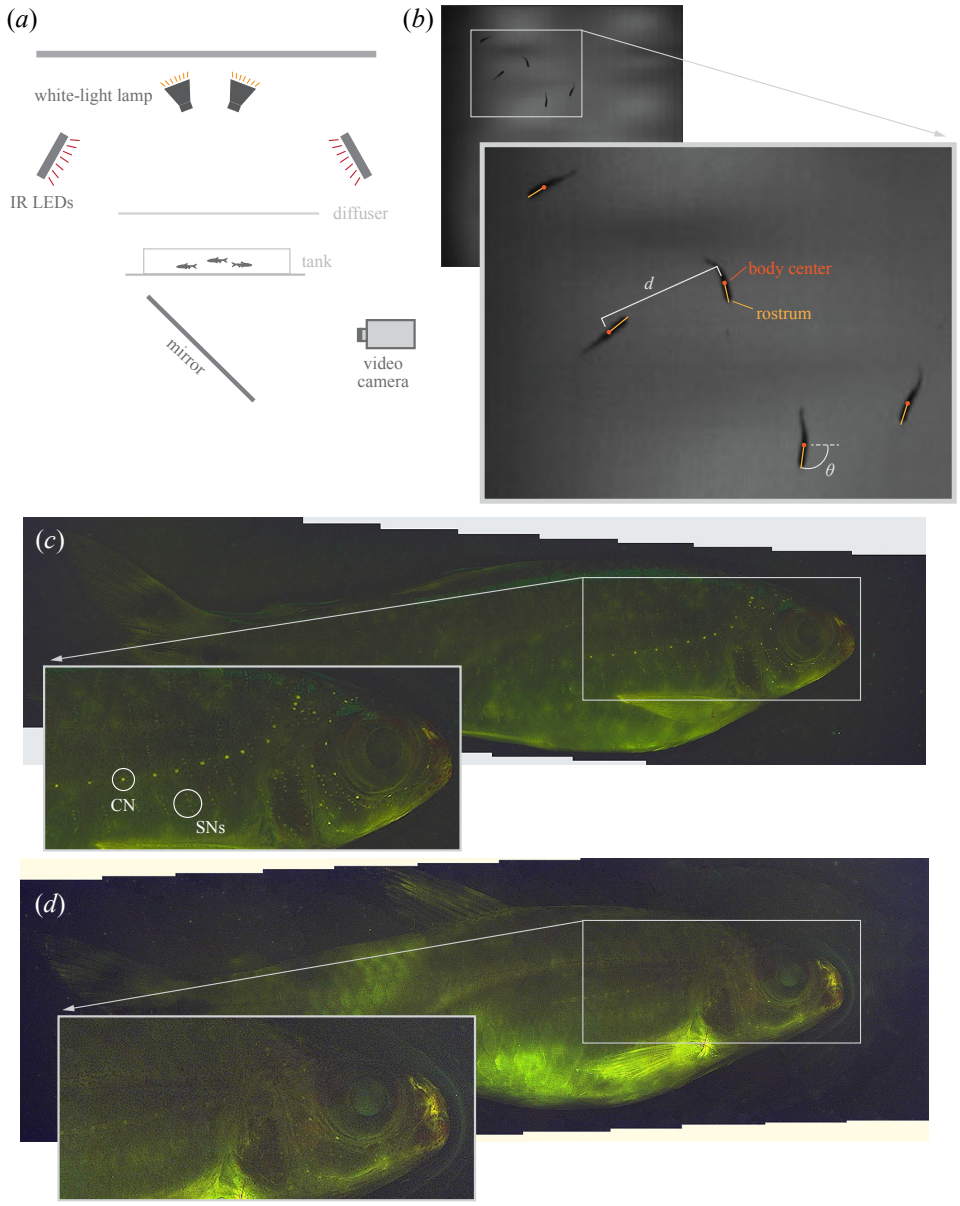

Figure B.1: Kinematic measurements and experimental manipulation of the lateral line system. (a) Groups of 5 fish were recorded in an experimental tank that was illuminated with IR lights that were directed toward a diffuser, placed above the tank. Visible lights were directed toward the ceiling to provide reflected ambient illumination. (b) A video still of one of our high-speed recordings, which demonstrates the high contrast of the fish with the transmitted illumination provided by the IR lights. The inset highlights the automatic tracking of the positions of the body center and rostrum of each fish and illustrates measurements of the nearest-neighbor distance (d) and heading (θ). (c) The hair cells of the lateral line were visualized with fluorescent dye (DASPEI), with canal neuromasts (CN) appearing as relatively large circles and groups of superficial neuromasts (SNs) visible as circles that are more faint and smaller. (d) After exposure to an antibiotic (neomycin sulfate), the lateral line neuromasts were greatly attenuated in the intensity of the fluorescent dye.

Manipulation of lighting

We tested how schooling varies with light intensity with long-duration recordings. We recorded swimming for 30 min at each of 8 levels of illuminance (0 lx, 0.44 lx, 0.62 lx, 0.66 lx, 0.70 lx, 1.25 lx, 1.80 lx, and 8.15 lx). The order of these recordings was randomized and each recording was preceded by an acclimation period ($30 - 60$ min) at the illuminance level for the recording. A preliminary analysis of our results indicated an inability of the fish to school at close proximity with a high polarized orientation at low light intensities (< 1.50 lx). This prompted us to focus subsequent experiments that tested the role of flow sensing on experiments performed under bright light (8.15 lx) and dim light (1.80 lx) that was still sufficient for schooling.

Lateral line manipulation

We tested the role of flow sensing in schooling by experimental manipulation of the lateral-line system through exposure to a solution of neomycin sulfate (Fisher BioReagents,Fair Lawn, NJ, USA). This is a common procedure for inducing cell death among lateral line hair cells that does not affect the inner-ear hair cells used for hearing and balance [39]. Groups of fish were placed in a neomycin solution (0.27 g Neomycin sulfate in 300 ml fish water, pH = 7.2) for an extended period (2 hr) in the dark to avoid bleaching the light-sensitive neomycin. The fish were moved to a series of three fresh water rinses, each for 3 min. This protocol was developed by verifying its effects on lateral-line hair cells, as assessed by the fluorescent vital stain DASPEI (2-(4-(dumethylamino)styryl)-N-ethylpyridinium iodide; Invitrogen, Eugene, OR, USA). Fish were placed in a DASPEI solution (0.01 g DASPEI per 100ml water) for 15 min before 3 rinses. We then anesthetized the fish by placing them in a tricaine methanesulfonate (MS-222, Finquel, Argent Chemical Laboratories, Redmond, WA, USA) solution (4.2ml concentrate MS-222 per 100ml water). We took pictures down

the entire length of the fish using a stereomicroscope (Zeiss Discovery V.20, Carl Zeiss, Thornwood, NY, USA) with a GPF filter set (450–490 nm), fluorescence illuminator (120 W Mercury Vapor Short Arc, X-Cite series 120q, Lumen Dynamics, Mississauga, ON, CA), and a camera (AxioCam HRc, Carl Zeiss). We allowed them to recover in a small holding tank of fresh fish water before returning them to a main tank. The photographs of DASPEI staining were later stitched together in Photoshop (v.21.0.3, Adobe, San Jose, CA USA).

Sample sizes

We replicated our experiments across multiple groups of 5 fish. We performed long-duration experiments at 8 levels of illuminance in 5 groups (i.e., 40 experiments with 25 fish). We tested the role of the lateral line system on long-duration kinematics in 4 treated groups and 4 control groups, each of which we tested for differences between dim (1.80 lx) and bright (8.15 lx) light (i.e., 32 experiments with 40 fish). Therefore, we performed a total of 72 long-duration experiments on 65 fish. Short-duration experiments were performed on 8 control groups and 8 treated groups. This included the 40 fish used for the long-duration experiments and added an additional 40 fish (20 control in 4 groups, 20 treated in 4 groups). We performed 3 experiments under dim light and 6 under bright light for each of these groups. Due to the challenge of tracking individual fish over the entirety of an experiment, we successfully analyzed 141 out of the 192 short-duration experiments that were completed.

Automated acquisition of kinematics

We automated the acquisition of positional data of fish from our video with custom software. This process, and all other aspects of data analysis, was performed with scripting in Matlab (R2018b, MathWorks, Natick, MA, USA) with the Computer Vision and Statistics Toolboxes. Our software calibrated the videos in a manner that corrected for radial lens

distortion from video stills of a checkerboard placed at a variety of positions in the field of view (using the 'estimateCameraParameters' function). We differentiated the fish from the background first by calculating a single image from a video recording that appeared like an empty tank. This background image was determined by finding the 90% quantile value of each pixel across 100 frames that spanned each recording. Each video frame to be analyzed was inverted and we subtracted the pixel values of the inverted background image to yield an image of the video frame that isolated the moving fish, an image that we contrast-enhanced. The fish bodies were then identified by thresholding the processed images and filtering the resulting binary blobs by area. Occlusions, when one fish obstructs the view of another, were identified by an increase in blob area and frames that found fewer fish than the known number were rejected. The major axis of each blob served to identify the central orientation of the trunk and we evaluated the pixel values along the major axis and found that the anterior direction consistently included darker pixel values within a quarter of the body length from the centroid. We found the anterior margin of the rostrum by the spatial increase in pixel intensity in the anterior direction along the major axis. The posterior midline of the body was identified by first calculating the distance map of the blob. We then found the caudal peduncle as the highest pixel intensity in the posterior quadrant at the radial position from the body center at 0.4 times the major axis length.

Analysis of high-speed recordings

Our high-speed recordings provided the opportunity to track individuals over time and to glean detailed kinematics of swimming for each fish. This first required post-processing of the positional data where individuals across frames were initially identified as the closest centroid between consecutive frames. Occlusions and any other frames where the acquisition failed to find the known number of blobs presented gaps in temporal record for the positional data. These periods were neglected by our analysis if they occurred at the start or end of a

recording. Otherwise, we used the closest last known coordinate to link individuals across gaps in the data and filled the gap by linear interpolation over the interval.

A preliminary analysis revealed that the duration of bouts of intermittent swimming could be identified by large accelerations and decelerations. We calculated the speed of individuals (v) from the discrete difference in centroid position and low-pass filtered the data with a moving average over 20 video frames. Our software identified these events from a discrete calculation of acceleration from our speed measurements, additionally filtered by a moving average of speed values across 30 frames. In an effort to characterize intermittent swimming kinematics, we examined relationships between the duration of swimming bouts, periods of rest between bouts, and both the change in speed and mean speed of swimming. In addition, we examined relationships in mean values of the change in speed, bout duration, and rest duration between focal fish and the others in a school.

These kinematic variables were compared by generalized linear mixed-effects models. We treated the school number (i.e., particular groups of 5 fish) as a random effect and the lighting and lateral line treatment were treated as fixed effects. For example, the mean change in speed over swimming bouts ($\overline{\Delta v}$) was modeled as a function of burst duration (T_{burst}) as follows:

$$\overline{\Delta v} \sim 1 + T_{\mathrm{burst}} + \mathrm{treat}_{\mathrm{neo}} + \mathrm{light}_{\mathrm{dim}} + (1|\mathrm{school}), \tag{B.1}$$

where $\mathrm{treat}_{\mathrm{neo}}$ is a categorical variable (neomycin compared to control), $\mathrm{light}_{\mathrm{dim}}$ is another categorical variable (dim compared to bright), and school is the number of a particular school. Eqn. B.1 is offered in Wilkinson notation [93]. We used generalized linear mixed-effects models to test the magnitude of turning and changes in speed during the burst phase. However, this analysis considered how changes in heading and speed varied with the position of neighboring fish and therefore permitted the opportunity for multiple measurements from a single experiment. We therefore categorized turns by the number of fish to the left or

right of the focal fish and consequently treated the experiment number and fish number as additional random effects in our model. Our analysis of changes in speed considered the number of fish ahead and behind a focal fish, which allows for multiple measurements that were also addressed by experiment number and fish number as random effects.

Analysis of long-duration recordings

Positional data provided the basis for measurements of kinematics from our long-duration recordings. Centroid tracking yielded sufficient measurements to satisfy the aim of the time-lapse recordings, which was to measure shoaling kinematics for groups, which did not require tracking individual fish over time. These measurements included the speed (V), nearest-neighbor distance (D), and polarization (ρ) of the group of fish. Speed was calculated as the discrete positional change in the mean coordinates of the group in each frame, divided by the change in time. The nearest neighbor at each time was identified as the minimum distance between each focal fish and the other fish in a school. As detailed in "Materials and methods", polarization offered a non-dimensional measure of the degree to which animals were oriented in the same direction, with possible values ranging from 0 to 1.

We compared mean values of kinematics over time between our experimental groups. These four groups were defined by bright and dim light and whether the fish had been treated with neomycin ('No lateral line') and the control. The comparison was performed as a two-way ANOVA with post-hoc comparisons performed by Fisher's least significant difference procedure [60, 44]. The post-hoc test included a consideration of an interactive effect between illuminance and flow sensing.

Results

Tables

Table B.1: Generalized linear mixed-effects modeling for change in heading (figure 2*b*). CI, 95% confidence interval; SE, standard error; tStat, t-Statistic; DF, degrees of freedom; n_{toward}, number of fish toward turn; $\text{treat}_{\text{neo}}$, neomycin treatment; $\text{light}_{\text{dim}}$, dim light. Model in Wilkinson notation [93]: $|\Delta\theta| \sim 1 + n_{\text{toward}} + \text{treat} + \text{light} + (1|\text{school}) + (1|\text{experiment}) + (1|\text{fish})$.

	coefficient						
variable	estimate	lower CI	upper CI	SE	tStat	DF	*P*
(intercept)	19.6	15.79	22.38	1.93	10.12	630	**¡ 0.001**
n_{toward}	1.95	0.93	2.97	0.52	3.74	630	**¡ 0.001**
$\text{treat}_{\text{neo}}$	-2.28	-5.98	1.41	1.88	-1.21	630	0.22
$\text{light}_{\text{dim}}$	-4.33	-7.30	-1.37	1.51	-2.87	630	**0.004**

Table B.2: Generalized linear mixed-effects modeling for change in speed (figure B.2). CI, 95% confidence interval; SE, standard error; tStat, t-Statistic; n_{ahead}, number of fish ahead; $\text{treat}_{\text{neo}}$, neomycin treatment; $\text{light}_{\text{dim}}$, dim light. Model in Wilkinson notation [93]: $|\Delta v| \sim 1 + n_{\text{ahead}} + \text{treat} + \text{light} + (1|\text{school}) + (1|\text{experiment}) + (1|\text{fish})$.

	coefficient						
variable	estimate	lower CI	upper CI	SE	tStat	DF	*P*
(intercept)	5.31	4.25	6.37	0.54	9.88	629	**¡ 0.001**
n_{ahead}	0.21	0.01	0.41	0.10	2.08	629	**0.04**
$\text{treat}_{\text{neo}}$	-0.08	-1.32	1.17	0.64	-0.12	629	0.90
$\text{light}_{\text{dim}}$	-0.41	-0.29	1.11	0.36	1.16	629	0.25

Table B.3: Generalized linear mixed-effects modeling for speed, burst duration, and coast duration (figure B.4). CI, 95% confidence interval; SE, standard error; tStat, t-Statistic; DF, degrees of freedom; $\overline{\Delta v}$, mean change in speed (cm s^{-1}); $\overline{v}$, mean speed (cm s^{-1}); T_{coast}, coast duration (s); T_{burst}, burst duration (s); $\text{treat}_{\text{neo}}$, neomycin treatment; $\text{light}_{\text{dim}}$, dim light. Models shown in Wilkinson notation [93].

	coefficient						
variable	estimate	lower CI	upper CI	SE	tStat	DF	P
$\overline{\Delta v} \sim 1 + T_{\text{burst}} +$ treat + light + (1—school)							
(intercept)	-1.69	-3.87	0.50	1.10	-1.53	123	0.13
T_{burst}	52.92	38.36	63.48	6.34	8.03	123	**¡ 0.001**
$\text{treat}_{\text{neo}}$	-0.14	-1.41	1.13	0.64	-0.22	123	0.82
$\text{light}_{\text{dim}}$	0.09	-0.86	1.04	0.48	0.19	123	0.85
$\overline{v} \sim 1 + T_{\text{burst}} +$ treat + light + (1—school)							
(intercept)	4.11	1.69	6.53	1.22	3.36	123	**0.001**
T_{burst}	9.69	-2.26	21.63	6.03	1.61	123	0.11
$\text{treat}_{\text{neo}}$	-0.77	-2.92	1.38	1.09	-0.71	123	0.48
$\text{light}_{\text{dim}}$	2.18	-1.29	3.08	0.45	4.82	123	**¡0.001**
$T_{\text{coast}} \sim 1 + T_{\text{burst}} +$ treat + light + (1—school)							
(intercept)	0.79	0.59	0.99	0.10	7.80	121	**¡0.001**
T_{burst}	-1.03	-2.15	0.08	0.56	-1.84	121	0.07
$\text{treat}_{\text{neo}}$	0.07	-0.06	0.20	0.07	1.03	121	0.31
$\text{light}_{\text{dim}}$	-0.17	-0.25	-0.08	0.04	-3.86	121	**¡0.001**
$\overline{v} \sim 1 + T_{\text{coast}} +$ treat + light + (1—school)							
(intercept)	8.31	6.58	10.04	0.88	9.49	124	**¡0.001**
T_{coast}	-4.23	-6.01	-2.44	0.90	-4.69	124	**¡0.001**
$\text{treat}_{\text{neo}}$	-0.49	-2.25	1.28	0.89	-0.54	124	0.59
$\text{light}_{\text{dim}}$	1.29	-0.39	2.19	0.45	2.85	124	**0.005**

Table B.4: Generalized linear mixed-effects modeling for relationships in kinematics between focal fish and other fish (figure B.5). CI, 95% confidence interval; SE, standard error; tStat, t-Statistic; DF, degrees of freedom; $\overline{\Delta v}$, mean change in speed (cm s^{-1}); T_{coast}, coast duration (s); T_{burst}, burst duration (s); $\text{treat}_{\text{neo}}$, neomycin treatment; $\text{light}_{\text{dim}}$, dim light. Models shown in Wilkinson notation [93].

	coefficient						
variable	estimate	lower CI	upper CI	SE	tStat	DF	P
$\overline{\Delta v}_{\text{focal}} \sim 1 + \overline{\Delta v}_{\text{other}}$+ treat + light + (1—school)							
(intercept)	1.62	0.35	2.89	0.64	2.53	126	**0.01**
$\overline{\Delta v}_{\text{other}}$	0.67	0.49	0.85	0.09	7.53	126	**¡ 0.001**
$\text{treat}_{\text{neo}}$	-0.14	-1.04	0.76	0.45	-0.31	126	0.76
$\text{light}_{\text{dim}}$	0.78	-0.02	1.57	0.40	1.93	126	**0.05**
$T_{\text{coast,focal}} \sim 1 + T_{\text{coast,other}}$+ treat + light + (1—school)							
(intercept)	0.32	0.09	0.55	0.12	2.76	119	**0.006**
$T_{\text{coast,other}}$	0.53	0.19	0.87	0.17	3.07	119	**0.002**
$\text{treat}_{\text{neo}}$	0.01	-0.13	0.14	0.07	0.10	119	0.92
$\text{light}_{\text{dim}}$	-0.05	-0.20	0.10	0.07	-0.67	119	0.50
$T_{\text{burst,focal}} \sim 1 + T_{\text{burst,other}}$+ treat + light + (1—school)							
(intercept)	0.08	0.05	0.12	0.02	4.45	121	**¡0.001**
$T_{\text{burst,other}}$	0.44	0.21	0.67	0.11	3.85	121	**¡0.001**
$\text{treat}_{\text{neo}}$	0.002	-0.010	0.013	0.006	0.30	121	0.77
$\text{light}_{\text{dim}}$	0.010	0.001	0.023	0.005	2.18	121	0.03

Additional figures

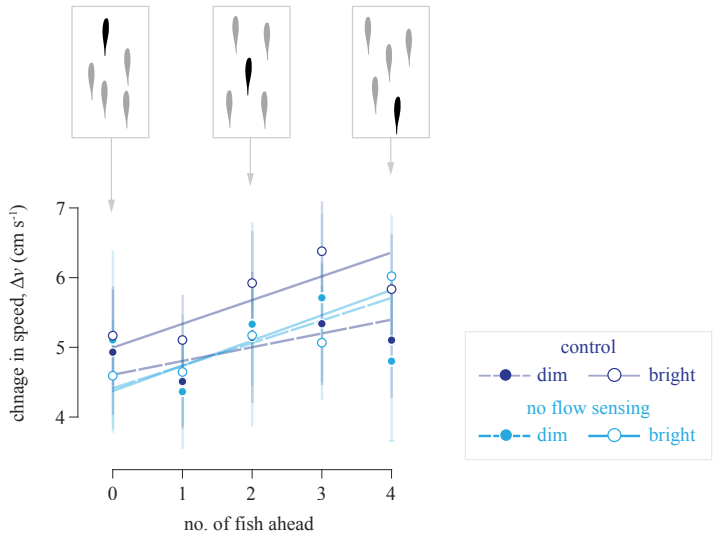

Figure B.2: Change in speed during the burst phase, relative to the number of fish ahead and behind the focal fish. Measurements are shown for four neomycin-treated (i.e., 'no flow sensing', red, $n = 8$) and control (blue, $n = 8$) groups under dim (1.80 lx, filled circles) and bright (8.15 lx, open circles) light for 141 experiments, with analysis of all 5 individuals from each group. Mean values are plotted with 95% confidence intervals that assume a normal distribution. The line shows the linear relationship with respect to the position of neighboring fish ($r^2 = 0.60$). Our generalized linear mixed-effects model found no significant effects of illuminance and the lateral-line treatment (table B.2).

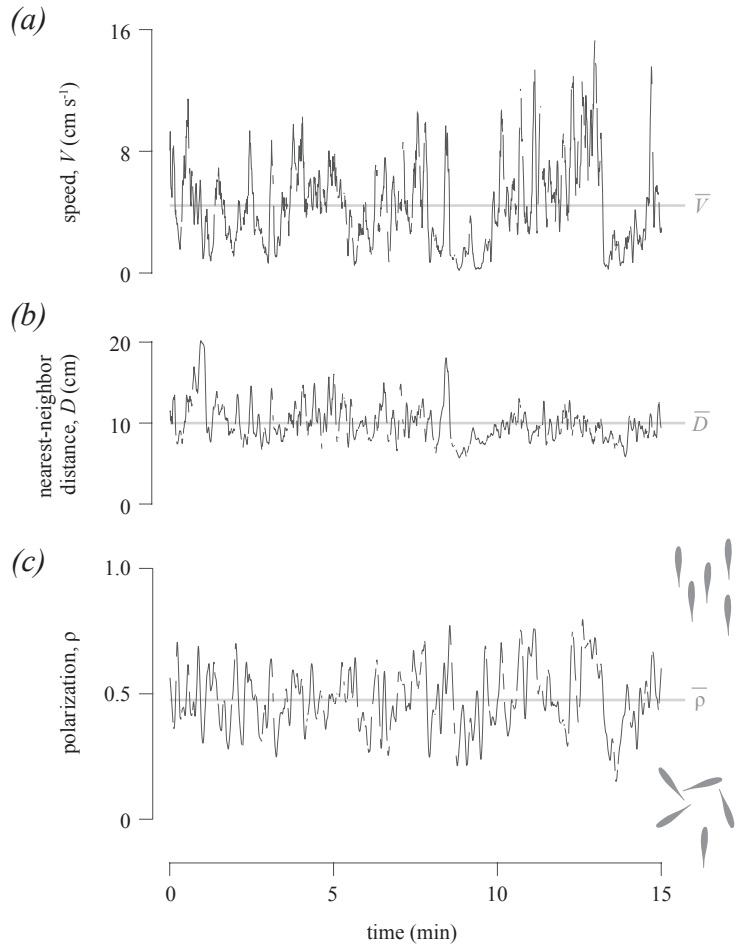

Figure B.3: Representative long-duration kinematic measurements, as recorded by time-lapse (0.5 frames s^{-1}) videography. (*a*–*c*) Schooling kinematics for a group of 5 fish, as measured by mean values among the members for the (*a*) speed, (*b*) nearest-neighbor distance, and (*c*) polarization for swimming at a fixed light intensity (8.15 lx). Speed and distance were calculated as the mean value at each time among all individuals. Polarization was calculated at each time by integration among the group members (Eqn. 2.1) and the schematic to the right illustrates two groups of fish with at extreme values of polarization. The mean values (gray horizontal line) are highlighted in each panel. These plots show half of the duration of a full (30 min) experiment to visualize the temporal variation. Gaps in the traces correspond to frames where occlusions or other failures in tracking occurred.

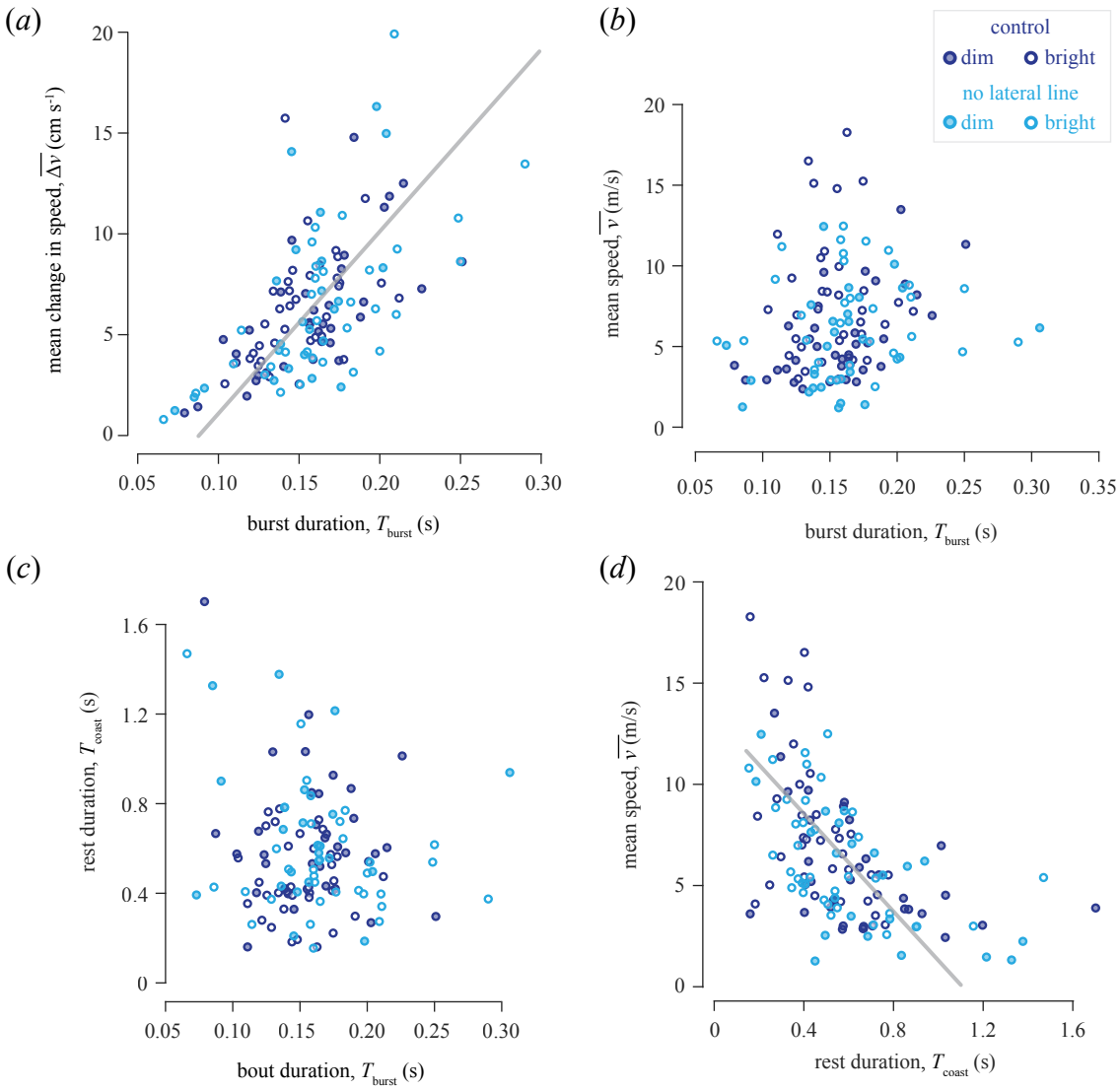

Figure B.4: The change in speed during a burst of swimming ($\overline{\Delta v}$) and the time-averaged mean speed ($\overline{v}$) are shown with respect to the duration of swimming bursts (T_{burst}) and the periods of coasting (T_{coast}) between bouts for 127 experiments conducted for control ($n = 8$) and neomycin-treated ($n = 8$) groups (5 fish per group). Each symbol represents the mean value for 3 or more bouts of swimming among a unique group of 5 fish in an individual experiment. The legend in the upper-right differentiates the symbols by the 4 experimental treatment groups. Trend lines are shown for the significant factors, according to our generalized linear mixed-effects model (table B.3). (a) Variation in the mean change in speed is positively related to the bout duration ($r^2 = 0.34$). No such relationships were found between (b) bout duration and mean speed ($r^2 = 0.03$) or (c) bout duration and rest duration ($r^2 = 0.02$). However, (d) a negative relationship was found between rest duration and mean speed for experiments under dim light (1.80 lx, solid line, $r^2 = 0.26$) and bright light (8.15 lx, dashed line, $r^2 = 0.26$).

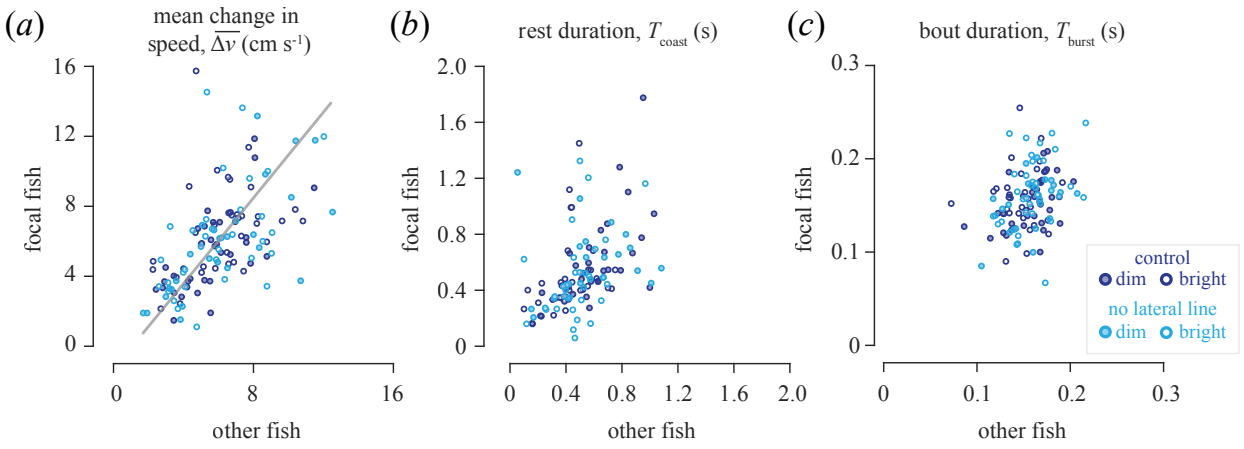

Figure B.5: Relationship in kinematic parameters between focal fish and the other members of a school. Each symbol represents the mean value for 3 or more bouts of swimming among a unique group of 5 fish in an individual experiment ($n = 130$). The legend (right side) differentiates the symbols by the 4 experimental treatment groups. (a) Variation in speed by focal fish is partially predicted by the speed of others for experiments under dim light (1.80 lx, solid line, $r^2 = 0.52$) and bright light (8.15 lx, dashed line, $r^2 = 0.18$). Less of the variation in (b) rest duration ($r^2 = 0.09$), or (c) the bout duration ($r^2 = 0.10$) of focal fish may be predicted by those variables in neighboring fish. See table B.4 for the results of generalized linear mixed-effects modeling.